MASTERARBEIT / MASTER'S THESIS

Titel der Masterarbeit / Title of the Master's Thesis

„Life in a tube: Morphology of the ctenostome bryozoan *Hypophorella expansa*."

verfasst von / submitted by

Philipp Pröts BSc

angestrebter akademischer Grad / in partial fulfilment of the requirements for the degree of

Master of science (MSc)

Wien, 2018 / Vienna, 2018

Studienkennzahl lt. Studienblatt / degree programme code as it appears on the student record sheet:	A 066 831
Studienrichtung lt. Studienblatt / degree programme as it appears on the student record sheet:	Masterstudium Zoologie
Betreut von / Supervisor:	Univ.-Prof. DDr. Andreas Wanninger

Abstract

Bryozoa (=Ectoprocta) is a large lophotrochozoan clade and consists of colonial aquatic filter-feeders. The boring ctenostome *Hypophorella expansa* inhabits parchment-like polychaete tubes. Its life-style and unique habitat calls for a detailed morphological analysis to assess morphological adaptations. To this end, immunostaining and confocal laser scanning microscopy (CLSM), histology and transmission electron microscopy (TEM) were used. The colony of *H. expansa* is composed of elongated stolons with a distal capsule-like expansion of the cystid wall which possesses a median transversal muscle; one autozooid is laterally attached to a capsule. Autozooids possess two fronto-lateral spherical structures on the body wall that provide space inside the tube ("space balloons"). A distal gnawing apparatus is present to perforate the polychaete tube wall. A muscular net of the tentacle sheath originates at the lophophoral base and condenses into four parieto-vaginal bands. The digestive tract consists of a myoepithelial pharynx, a short esophagus and cardia, a bulbous caecum, an elongated intestine and a distally terminating anus. The cerebral ganglion on the anal side of the lophophoral base innervates tentacle sheath, lophophore and foregut. Four tentacle sheath neurite bundles emerge from the cerebral ganglion and distally fuse into two; each tentacle is innervated by three frontal and one abfrontal tentacle neurite bundle. The growth pattern of the colony of *H. expansa* may provide a fast colonization of the polychaete tube layers. Helicoidally arranged tentacle sheath musculature probably provides stability without the need of additional circular muscle fibers. The musculature associated with the gnawing apparatus is considered homologous to the vestibular wall musculature of ctenostome species. During bryozoan evolution the tentacle sheath innervation changed from short neurite bundles that dissociate into a nerve plexus in Phylactolaemata to two distinct tentacle sheath neurite bundles that prevail over the whole distance of the tentacle sheath in Gymnolaemata. The medio-lateral visceral neurite bundles of

ctenostomes may be homologous to the medio-lateral neurite bundles of phylactolaemates. Based on comparative data the last common ancestor of Gymnolaemata probably possessed two striated tentacle myofibrils, parietovaginal bands, a pharyngeal myoepithelium, longitudinal intestinal myofibrils, a proximally positioned anus, few distinct tentacle sheath neurite bundles that further innervate the aperture and parietal muscles, four tentacle neurite bundles of which the mediofrontal neurite bundle emerged directly from the circumoral nerve ring and a distinct medioviscerial neurite bundle.

Introduction

Bryozoa is a phylum of aquatic colonial filter feeders within the Lophotrochozoa. It consists of three major clades, Phylactolaemata, Gymnolaemata and Stenolaemata. Phylactolaemata contains freshwater forms with body wall musculature, an epistome (a lip-like structure protruding over the mouth opening) and a horseshoe-shaped lophophore. The calcified cyclostomes are the only extant clade of Stenolaemata and are marine; they possess a circular lophophore and a membranous sac, which is a peritoneal coating of the polypide that is separated from the epidermis (Mukai et al., 1997). The mainly marine Gymnolaemata contains two clades, the noncalcified paraphyletic ctenostomes and the monophyletic calcified cheilostomes that possess an operculum and arose from a ctenostome-like ancestor (Todd, 2000; Waeschenbach et al., 2012). Two basic colony growth patterns are known in ctenostomes which have been used in the past to define two distinct taxa called "Carnosa" and "Stolonifera". Today, these names are merely polyphyletic terms to describe colony morphology types of ctenostomes: "Carnosa" show a flat compact colony growth pattern whereas "Stolonifera" possess interconnecting branching stolons that are separated via septal pore plates and bear feeding autozooids (Mukai et al., 1997).

Ctenostomes show relatively little diversity with only around 300 extant species compared to over 5000 cheilostomes (Waeschenbach et al., 2012). Only a small portion of the 300 ctenostome species exhibit a boring life style.

Hypophorella expansa Ehlers, 1876, is a boring "stoloniferan" ctenostome, possesses a mechanical gnawing apparatus and constitutes the only known member of the Hypophorellidae. Its creeping stolons bear a median tranversal muscle inside their distal ends and are succeeded by one distally attached autozooid (lateral position) and two additional distal stolons (one in lateral position, one in terminal position). *H. expansa* is placed inside the Walkerioidea. There are two known boring strategies, the first uses chemical substances to bore through mostly calcareous structures such as molluscan shells, while the second one uses a mechanical gnawing apparatus (Pohowsky, 1975; Pohowsky, 1978). The colony of *H. expansa* spreads underneath the layers of parchment-like tubes secreted by polychaete annelids such as *Lanice conchilega* (Ehlers, 1876) and *Chaetopterus* sp. The fertilized eggs develop into cyphonautes larvae, which are released into the tube lumen, settle at the inner-most surface of the polychaete tube and develop further into a kenozooidal stolon (Ehlers, 1876). The rest of the colony (autozooids and succeeding stolons) forms by asexual budding. Once the colony is covered with a newly secreted polychaete tube layer, the gnawing apparatus of the autozooids perforate this layer towards the tube lumen, enabling the lophophores to be everted for feeding.

Considering the unique habitat of *H. expansa* and boring bryozoans in general, the emergence of remarkable morphological adaptations (autapomorphies) is not surprising. Besides the gnawing apparatus of the autozooids, both the feeding autozooids and the interconnecting stolons of the colony show very conspicuous cystid structures that may play a role in providing space and stability for the entire colony. The feeding types show distal spherical structures at the fronto-lateral side of their cystids (Ehlers, 1876; Joyeux-Laffuie, 1888; Prouho, 1892). Stolons possess peculiar wrinkles in its elongated proximal part of the cystid wall. Both morphological peculiarities are not known in any other "stoloniferan" bryozoan.

Live colonies of *H. expansa* were found and collected from the Mediterranean Sea. Prior to this study, investigations of *H. expansa* were limited to light microscopical studies (Ehlers, 1876), thus calling for re-analyses using modern methods. Therefore, the present study employs histological, immunocytochemical and ultrastructural methods to revisit this unique bryozoan in order to gain a better understanding of its morphology and adaptations to its extraordinary lifestyle.

Materials and methods

Animals and fixation

Chaetopterus sp. tubes inhabited by colonies of *Hypophorella expansa* were collected from 30 meter depth from a secondary hard-bottom using a dredge in July 2015 in Rovinj, Croatia. For transmission electron microscopy (TEM), parts of the samples were fixed in 2.5% glutaraldehyde in 0.1 M cacodylate buffer (pH = 7.4) with 10% sucrose added. After several washes the samples were postfixed in 1% Osmium tetroxide in double-distilled water for one hour and dehydrated in acidified dimethoxypropane. Specimens were infiltrated and embedded in low viscosity resin (Agar Scientific Ltd., Essex, United Kingdom) for semi- and ultrathin sectioning. For immunocytochemistry (ICC) samples were fixed in 4% paraformaldehyde in 0.1 M phosphate buffer for one hour at room temperature, rinsed 3-4 times in phosphate buffer, and stored in phosphate buffer for subsequent analysis.

Immunocytochemistry and confocal microscopy

Antibody, phalloidin and nuclei staining

Specimens were dissected from the tubes prior to staining. The extracted parts of the colony were then transferred into a solution of 0.1 M phosphate buffer with 2% TritonX (PBT), 2% DMSO and 6% NGS for blocking and permeabilization overnight. Samples were then blocked in PBT-NGS-DMSO solution (PND) and incubated for 24 hours in a monoclonal anti-mouse acetylated α-tubulin primary antibody (dilution 1:800) in PND and kept at room temperature in the dark overnight. Subsequently, the samples were rinsed thrice for 30 minutes each in PBS and afterwards incubated for 24 hours in secondary antibody goat anti-mouse Alexa Flour 568 (Molecular Probes, Eugene, OR) (dilution 1:300 in PND). Afterwards, samples were rinsed three times for around 30 minutes in PBS. DAPI (Invitrogen, Carlsbad, CA, USA) in a dilution of 1:120 was added to label cell nuclei; f-actin filaments were labeled with Alexa Flour 488 phalloidin (Molecular Probes, Eugene, OR) in a dilution of 1:60. Subsequently, samples were rinsed three times for 30 minutes each and afterwards mounted on standard microscope slides with Fluoromount G (Southern Biotech, Birmingham, AL, USA). The slides were kept at 4°C for 1-2 days prior to examination.

Analysis and image acquisition were performed on a Leica SP5 II confocal scanning microscope (Leica Microsystems, Wetzlar, Germany). Confocal image stacks were acquired with the LAS AF Software using 0.5 at 1 μm slice thickness. The ImageJ package Fiji (Schindelin et al., 2012) and Drishti (Ajay Limaye, 2012) were used for further image processing.

Transmission electron microscopy (TEM) and light microscopy

Sample preparation

Semi- and ultra-thin sections (1 μm and 60 nm thickness respectively) were produced with a LEICA UC6 microtome (Leica Microsystems, Wetzlar, Germany). For TEM, ultra-thin sections were transferred onto copper grids and contrasted with uranyl-acetate for 30 minutes and dipped

in 3 cups with double-distilled water for 15 times each. Thereafter the samples were contrasted in lead-citrate for 5 minutes, rinsed as described above and the remaining liquid was removed using filter paper. Alternatively, samples were contrasted in a gadolinium-III-acetate (30 minutes) instead of uranyl acetate followed by lead-citrate (5 minutes) and rinsed as mentioned above. Analysis and image acquisition was performed on a TEM Zeiss Libra 120 electron microscope (Carl Zeiss AG, Oberkochen, Germany) equipped with the software iTEM.

Semi-thin sections were stained with toluidine blue for 10-15 seconds at 65°C and mounted in low viscosity resin. Image acquisition was conducted with a Nikon Eclipse E800 light microscope (Nikon, Chiyoda, Tokio, Japan) and a Nikon Fi2-U3 camera.

Results

Colony overview

Inside the housing tubes of the polychaete *Chaetopterus* live colonies of *Hypophorella expansa* were found. The bryozoan colony consists of elongated branch-like stolons with attached feeding autozooids (Figs 1, 2). Both autozooids and stolons are composed of two basic parts: a cellular endocyst (cellular linings) that is surrounded by a completely transparent, possibly chitinous ectocyst (also cystid or body wall). Autozooids also possess a polypide that consists of musculature, a lophophore and a U-shaped gut. Autozooids and stolons are separated from each other via pore plates (Fig. 1 B, Fig. 2 A-C). Stolons bear an autozooid at their lateral distal ends, a succeeding stolon at their terminal ends and an attached lateral stolon opposite of the lateral autozooid (Fig. 1 B, D). The colony grows between the layers of the polychaete tube wall. A fully developed stolon possesses a slim elongated wrinkled proximal part and a distal, smooth part with a capsule-like expansion (Fig. 2 A, B, E) on which a single autozooid is laterally

attached (Fig. 1 B, D). The proximal part of a succeeding stolon directly follows the distal capsule of a preceding stolon. The lateral position of autozooids of neighboring stolons alternates from left to right with respect to the proximal-distal-axis of the stolon.

Stolons

Structure of stolons

The stolons possess a body cavity which, in accordance with the width of the cystid wall, widens when approaching their distal capsules (Fig. 1 B, D; Fig. 2). At the proximal part of the stolon regular wrinkles are visible at the inner side of the ectocyst (Fig. 1 D; Fig. 2 A - D). The wrinkles protrude towards the median stolon axis and show a higher electron density than the connected cystid wall (Fig. 2 E). These possess a crescent-like shape and are positioned at the inner stolon wall, where they progress transversally from the frontal to the basal side with their endings occasionally ramifying (Fig. 2 A). The wrinkling is confined to the thin areas of the stolons and is not present at the proximal attachment or distal capsule-like site and show a higher electron density than the connected cystid wall (Fig. 2 A, B, E).

Each stolon is connected to both autozooid and neighboring stolon via a perforated septum (pore) (Fig. 1 B, Fig. 2 A-C). At the contact points of two neighboring stolons (and stolon and neighboring autozooid) the cystid walls turn medially. They form a small central perforation which is surrounded by a complex of three cell types that form a rosette: "special cells, "cincture cells" and "limiting cells" (after terminology of Gordon, 1975). This cell complex separates succeeding stolons and autozooids from their respective stolons (Fig. 2 C, D). Limiting cells are arranged hemispherically around the pore plates to form the outline of rosettes (Fig. 2 C, D), although these cell complexes are not present on the side of the autozooids. Cincture cells line the perforation of the cuticle in the rosette and turn medially where they project into the

neighboring stolon or autozooid (Fig. 2 D). Special cells are positioned between cincture cells and limiting cells. They show f-actin signal that projects through the pore between the flanking "cincture cells" (Fig. 2 C+D). This cell arrangement further serves as a communication/transport complex.

Stolon musculature

Stolon capsules possess several densely arranged muscles that run in a median position from the basal towards the frontal cystid wall: the smooth median transversal muscles (Fig. 1 B, D; Fig. 2 A, C, D, F). Their prominence and relatively dense arrangement resembles the parietal muscles of autozooids. Tendon cells are present at muscle attachment sites, connecting the muscle fibers via tonofilaments to the cystid wall (Fig. 2 F). The special cells of a rosette possess f-actin fibers, penetrate the perforation of the pore and get in contact with the special cells on the other side of the pore (Fig. 2 C, D).

Autozooids

Structure of autozooids

The autozooid has a completely transparent vase-like cystid wall and is attached proximally to the lateral side of the widened, distal stolon capsule, via a small flattened area on the baso-lateral side of the cystid (Fig. 1 B, D). Its polypide comprises a circular lophophore with 10-14 ciliated tentacles for food acquisition (Fig. 1 A, C, D; Fig. 3 B), muscle fibers for polypide movement, a U-shaped gut, a nervous system with a cerebral ganglion at the anal side of the lophophoral base and gametes in the body cavity close to the body wall. The disto-lateral parts of each autozooid bear two spherical cystid structures, the space balloons (Fig. 1 A, B, D; Fig. 3). Both ectocyst and space balloons show an acellular cuticle that is lined by an epidermal layer, which is thinner

inside the space balloons (Fig. 3). Pores that connect the fluid of the space balloons with the rest of the autozooidal body fluid were not detected. At the distal-most region of the cystid, a bulbous, lip-like expansion of the vestibulum bears a bipartite gnawing apparatus consisting of several ridges of columns with pointed (probably chitinous) teeth at their tips (Fig. 4 A-C). When the polypide is retracted the lip structure partially covers the orifice. In this area, the vestibular wall continues proximally into the tentacle sheath which extends into the lophophoral base where the mouth opening is situated. It leads into a muscular pharynx that continues into a tube-like esophagus (Fig. 1 A, B; Fig. 5 C, D, E). It terminates with a cardiac valve, which marks the beginning of the tube-like cardia. The latter continues into a bulbous caecum (Fig. 1 B, Fig. 5 B, E, F). The caecum continues distally into a highly ciliated cup-like pylorus with a distally succeeding elongated intestine (Fig. 1 B, Fig. 5 A, Fig. 6). At the proximal caecal end, a very delicate funiculus extends proximally through the body cavity and inserts near the pore plate that connects the autozooid with its corresponding stolon (Fig. 5 A, B). The intestine terminates with an anus at the distal end of the tentacle sheath (Fig. 1 A, B, D; Fig 5 A). Some autozooids show rows of cilia running along the anal side of the surface of the foregut towards the lophophoral base, where a supraneural coelomopore is present (Fig. 7). Other autozooids lacked these structures (Fig. 7 D). In some of the autozooids developing eggs and sperm were present. Testes are placed laterally at the inner proximo-lateral side of the autozooidal cystid (Fig. 8 A). In early development spermatogonia are clustered in spherical complexes (Fig. 8 A). Free-floating spermatocytes are later present throughout the entire body cavity (Fig. 8 A). The ovaries show a distinct placement at the median side of the parietal musculature (Fig. 8 B, C). Ovaries and testes were not present simultaneously in the same autozooid. Tentacles possess a coelom at their tips (Fig. 9 E). The tentacle epidermis consists of one frontal, two latero-frontal, two lateral, two latero-abfrontal and one abfrontal cells (Fig. 10 B, C). Cilia rootlets are present in latero-frontal, lateral and latero-abfrontal cells (Fig. 10 B, C).

Autozooidal musculature

Apertural musculature

Depending on whether the lophophore is retracted or protruded, the relative position of the tentacle sheath, diaphragmatic sphincter and the vestibular wall musculature differs (Fig. 11). The muscle apparatus of the apertural area contains several muscle bundles. The diaphragm at the connection between the vestibular wall and tentacle sheath has several concentrically arranged ring muscles. When the lophophore is protruded, these are located distally of the vestibular wall musculature (Fig. 11 C, D). The muscles of the parieto-diaphragmatic muscle bundles insert laterally at the body wall (Fig. 11 A). The musculature of the vestibular wall consists of several densely arranged ring muscles (Fig. 11 B, C, D). In protruded animals, two short muscle bundles traverse diagonally from the lateral attachment sites of the vestibular wall musculature towards the median axis of the gnawing apparatus (Fig. 11 C). Three additional groups of muscle bundles originate from the lateral side of the vestibular wall musculature. The lateral parieto-vestibular muscles progress towards the lateral body wall, the basal parieto-vestibular muscles towards the basal side of the body wall and the frontal parieto-vestibular muscles towards the fronto-distal side of the body wall (Fig. 11).

While the polypide is retracted, the diaphragmatic sphincter musculature is positioned basally of the vestibular wall musculature (Fig. 11 A). Additionally, the basal parieto-vestibular muscle fibers attach distally to the body wall on the basal side relative to the vestibular wall musculature (Fig. 11 A).

Tentacle sheath musculature

Between the epidermal and peritoneal layer of the tentacle sheath a net of oblique longitudinal muscle fibers originate at the lophophoral base and extends distally. These fibers further combine to four distinct muscle bundles and continue directly into the four parietovaginal bands

11

(Fig. 1 C; Fig 5 E; Fig. 9 B, Fig. 11 D). Two originate at the disto-latero-frontal side of the tentacle sheath and project towards the fronto-lateral body wall at the base of the space balloons (Fig. 1 C; Fig. 11 A, C, D). The other two originate on the baso-distal side of the tentacle sheath and continue towards the vestibular wall on the basal side of the cystid (Fig. 11 A).

Parietal muscles

The parietal muscles are situated laterally in the autozooidal body cavity and consist of a continuous row of densely arranged, smooth and transverse muscle bundles that emanate from the basal to the frontal cystid wall (Fig. 1 A-D, Fig. 5 F).

Lophophoral base and tentacle musculature

The pharynx consists of a prominent myoepithelium that is composed of densely arranged cross-striated circular muscles and several delicate longitudinal muscle strands (Fig. 1 C; Fig. 5 C, D). The mouth opening is positioned at its medio-distal end (Fig. 1 A, C; Fig. 5 C; Fig. 7 B). Perioral buccal dilatators extend from the pharynx into the ring canal where they attach to the outer lophophoral base below the median axis of each tentacle (Fig. 1 C; Fig. 5 D). At their base, two short lateral muscular tips are visible which possess a "V"-like shape (Fig. 5 E, F; Fig. 9 B). In between the base of each tentacle pair, abfrontally of the outer insertion of the buccal dilators, regular short smooth and circular muscle bundles, the basal transversal muscles, are present (Fig. 5 E, F; Fig. 9 A). Each tentacle possesses two longitudinal striated muscles (Fig. 9 B, C, E; Fig. 10 A). The basiepidermal extracellular matrix (ECM) forms a ring in cross section with two horn-like structures at the latero-abfrontal side (Fig. 10 A, B). This ring surrounds two distinct muscle bundles; one is positioned at the frontal and one at the abfrontal tentacle side (Fig. 10 A, B). Delicate circular muscle fibers are present on the tentacle tips (Fig. 9 C, D)

Gut musculature

The pharynx continues into a tube-like esophagus that shows slightly less dense and less prominent circular musculature (Fig. 1 C). A tight arrangement of epithelial cells, the cardiac valve, marks the border between the esophagus and the cardia (Fig. 5 B). The cardia shows regular loose smooth longitudinal and circular musculature and is separated from the bulbous caecum via a dense sphincter-like arrangement of ring musculature (Fig. 1 C; Fig. 5 B, D, E, F). The musculature of the caecum also consists of few loose smooth longitudinal and a higher number of smooth circular myofibrils (Fig. 1 C; Fig. 5 E, F). Distally, the caecum continues into a prominently ciliated pylorus that lacks musculature and separates the caecum from the ciliated intestine (Fig. 1 C; Fig 5 A; Fig. 6). Succeeding the pylorus distally, the elongated tube of the intestine has several delicate smooth longitudinal muscles (Fig. 1 C; Fig. 5 F) and extends into the distal part of the tentacle sheath, where the anus is positioned (Fig. 1 A, B, D; Fig 5 A, F).

Autozooidal nervous system

Cerebral ganglion

The center of the nervous system of an autozooid, the cerebral ganglion, is located at the anal side of the lophophoral base (Figs. 1 A, B; 5 A; 12; 13; 14 A, C; 15 A, B). It gives rise to a circumoral nerve ring that runs around the lophophoral base to its oral side (Fig. 12 A, Fig. 13 A, B). The ganglion itself innervates the tentacle sheath with 4 prominent tentacle sheath neurite bundles, the tentacles (in combination with the circum-oral nerve ring) and the pharynx with several visceral nerves (see below) (Fig. 12 B; Fig. 13).

Tentacle innervation

A different pattern of tentacle innervation is present on the oral and anal side of the lophophore, respectively (Figs. 13 A, B). On the anal side, the innervation has its origin on the disto-lateral sides of the cerebral ganglion (Fig. 13 A, Fig. 14 A). Four neurite bundles originate from each of these two lateral points from where the neurite bundles innervate the tentacles on the anal side, with the fourth neurite bundle (the lateral-most) giving rise to the origin of the circumoral nerve ring (Fig. 12 A; Fig. 13 A). Each of these eight prominent neurite bundles progress distally towards an intertentacular area and form the base of an intertentacular neural fork. Four neurite bundles innervate each tentacle: two frontolateral, one mediofrontal and one abfrontal neurite bundle (Fig. 13; Fig. 16). On the anal side all but the anal-most intertentacular fork provides neurite bundles for two neighboring tentacles. Two neurite bundles from two neighboring intertentacular forks emanate distally, converge medially and then join at the tentacle base, where they merge and continue as a single abfrontal neurite bundle throughout the tentacle. From the proximal side of two neighboring intertentacular forks two neurite bundles project towards the median, longitudinal axis of a tentacle and turn distally, where they fuse at the frontal side of each tentacle and continue along the tentacle as a single medio-frontal tentacle neurite bundle. A single neurite bundle originates from the intertentacular fork distally towards the frontal side of an intertentacular base, where it splits up and innervates two neighboring tentacles with one laterofrontal neurite bundle (Fig. 13 A). There is an exception to this regular innervation pattern, however. The anal-most tentacle receives its abfrontal innervation only from its corresponding intertentacular fork on the left side, whereas the medio-frontal nerve originates only from its corresponding intertentacular fork on the right side (Fig. 13 A). The tentacle innervation on the oral side shows a different situation (Fig. 13 B). On this side neurite bundles originate from the circumoral nerve ring and innervate the tentacles. The mediofrontal nerves originate from an intertentacular fusion of two neurite bundles that originate from the circumoral nerve ring at positions proximally of the intertentacular forks. These neurite bundles approach each other

while progressing distally to the frontal side, merge at the tentacle base and form a single medio-frontal tentacle neurite bundle. Both the abfrontal and latero-frontal tentacle neurite bundles originate from the distal ends of intertentacular forks, which originate from the same site as the previously mentioned neurite bundles that fuse to form the mediofrontal tentacle nerve (Fig. 13 B). From the circum-oral nerve ring they progress distally and give rise to intertentacular forks from where the abfrontal and latero-frontal neurite bundles originate. Such an intertentacular fork splits distally at the base of two neighboring tentacles, providing one latero-frontal neurite bundle for each. The previously described pattern of dual-origin of abfrontal tentacle neurite bundles (see above) does not apply to the oral side (Fig. 13 A, B). From the origin of the latero-frontal tentacle neurite bundles, a third splitting is present, that gives rise to an additional neurite bundle that progresses to the abfrontal side in disto-lateral direction where it provides only one tentacle with an abfrontal tentacle neurite bundle (Fig. 13 B). On the oral side tentacles on the left side of the lophophore are innervated by their preceeding left intertentacular fork by a single abfrontal tentacle neurite bundle each and vice versa for the right side. All observed autozooids had an uneven number of tentacles, which leads to the situation that one intertentacular fork on the oral side does not innervate tentacles with an abfrontal neurite bundle (Fig. 13 B). While progressing distally, latero-frontal and frontal neurite bundles approach each other (Fig. 11 A, C). It could not be clarified, whether these neurite bundles fuse further distally.

Tentacle sheath innervation

Four neurite bundles innervate the tentacle sheath (Fig. 12 B, Fig. 13 C, Fig. 14 C). One pair originates from the disto-lateral and the other from the proximo-lateral edge of the cerebral ganglion (Fig. 12 B, Fig. 13 C, Fig. 14 C). The proximal pair projects laterally where it splits into a distally traversing branch that innervates the tentacle sheath and a proximal branch that innervates the foregut laterally. The distal branch shows an additional perpendicular branch that partially encircles the tentacle sheath (Fig 13 C, Fig. 14 C). The second pair of tentacle sheath

neurite bundles progresses from the disto-lateral edge of the cerebral ganglion and continues diagonally to the lateral side of the tentacle sheath where it joins the distally traversing tentacle sheath neurite bundle that originates proximally (Fig. 13 C, Fig. 14 C). These two neurite bundles progress distally in close proximity and innervate the apertural/orificial area (see below).

Visceral innervation

Seven visceral neurite bundles in total emerge from the cerebral ganglion and innervate the foregut (Fig. 12 B; Fig. 15 A, B, C). From the proximal side of the cerebral ganglion, four neurite bundles progress proximally towards the foregut and approach each other to produce the prominent medio-visceral neurite bundle (Fig. 12 B, Fig. 13 C, Fig. 15 B, D). The prominent medio-visceral neurite bundle extends proximally towards the cardiac valve (Fig. 15 D). Two more delicate neurite bundles flank this prominent one and progress towards the cardiac valve, but whether they reach it could not be clarified (Fig. 15 B). Additionally, four latero-visceral neurite bundles are present, two on each lateral side of the foregut (Fig. 15 A, B, C).

Apertural and parietal innervation

The muscular apparatus of the aperture is innervated by tentacle sheath neurite bundles at the distal-most part of the tentacle sheath, where they project from the tentacle sheath distally (in case of a retracted lophophore) to the muscular apparatus of the aperture (Fig. 17 A). Additional neurite bundles extend from the distal tentacle sheath into the frontal parieto-vaginal bands to the base of the space balloons, where they turn proximally along the frontal body wall towards the parietal muscles and meander through the muscular strands (Fig. 17 A, B).

Discussion

In this work, phylogenetic analyses on ctenostomes based on morphological data are used for evolutionary considerations (Jebram, 1986; Todd, 2000 – Fig. 18 A, B respectively). In both studies, Alcyonidioidea and Hislopioidea are regarded as early branches, whereas the "stoloniferan" Walkerioidea and Vesicularioidea are later branches.

Colony of *Hypophorella expansa*

The analysis of the housing tube of *Chaetopterus* sp. revealed a colonial appearance of *Hypophorella expansa* as previously described (Ehlers, 1876). A stolon forms one single autozooid at most, which is attached laterally to the distal stolon capsule (Ehlers, 1876; Jebram 1973). The existence of kenozooidal stolons without attached autozooids is regarded as a form of division of labor (Jebram, 1973). The chief task of main branches is the dispersal of the colony itself, whereas the task of secondary branches is the formation of autozooids via budding (Jebram, 1973). *H. expansa* is placed inside the Walkerioidea, whose members possess autozooids either in median position (primary case of creeping stolons) or in lateral position (secondary state). Regarding the colony growth pattern, a laterally attached autozooid at the distal end of the creeping stolons of *H. expansa* is therefore regarded as an autapomorphy. An additional autapomorphy of *H. expansa* concerning the growth pattern is that autozooids of succeeding stolons are attached in an alternating manner regarding their lateral position (if the autozooid of a preceeding stolon is attached on the left side, the autozooid of the succeeding stolon is attached on the right side). An orthogonal branching of stolons probably results in an efficient dispersal of the colony to occupy a certain area. This growth pattern therefore may facilitate a rapid colonization of the polychaete tube.

Stolon structure

The peculiar wrinkling of the proximal part of an adult stolon of *Hypophorella expansa* is unique. A slightly comparable chitinous thickening of cystid walls is present in the autozooidal cystid walls in *Triticella flava* (Ehlers, 1876 (as *Triticella boeckii*); Hayward, 1985). In *T. flava* a chitinous hardening is present in the cystid wall of an autozooid (Hayward, 1985). In *H. expansa* there are numerous wrinkles, which occur only in the slim proximal parts of the stolons following the wrinkle-free attachment sites where the pore plates are situated (Ehlers, 1876). The presence of wrinkles, or chitinous hardenings in general, may provide higher stability to the cystid walls.

Autozooids and their corresponding stolons as well as two neighboring stolons are separated via a perforated septum, which is formed during the budding processes (Ehlers, 1876). The cells surrounding these septa from both sides form a rosette, which was previously reported (Ehlers, 1876) and which supposedly acts as a transport epithelium (Gordon, 1975). Previous assumptions concerning the existence of a closing membrane in these pores (Ehlers, 1876) can be rejected, since a similar cell complex around the septal perforation, in which special cells and cincture cells project through the perforation to the other side of the pore, as found in other gymnolaemates (Gordon, 1975; Mukai et al., 1997), are present. The rosette functions both as a mechanical plug and transport epithelium (Gordon 1975). The rosettes of the vesicularioidean ctenostome *Bowerbankia imbricata* were previously investigated in detail (Gordon, 1975). As a member of the Vesicularioidea it possesses a well-developed funicular system. In *H. expansa* only a very delicate funiculus is present in its autozooids. In contrast to previously reported funicular cords in the *H. expansa* (Ehlers, 1876) it is now known that the funicular system is absent in the stolons of this species and all other Walkerioidea (Jebram, 1973; and this work). It's highly likely that the detached body wall was previously observed within the cuticular lining of the stolon. Instead, a median transversal muscle is present in the distal stolon parts of Walkerioidea (not present in Vesicularioidea), which substitutes a stolonial funicular system

(present in Vesicularioidea). Such a muscle is also present during autozooidal development in the "carnosan" Paludicelloidea, which were reported previously as the ancestral group to Walkerioidea, which underwent a stolonisation process independentely (Jebram, 1973). The interrelationship of the ctenostome superfamilies is still obscure (Todd, 2000). In a recent phylogentic analysis, the Walkerioidea are placed inside a polytomy with Victorelloidea and Vesicularioidea as closest relatives (Todd, 2000). This situation with lack of a funicular system and a present median transversal muscle in Walkerioidea versus a present funicular system and no median transversal muscle in Vesicularioidea shows alternative strategies with respect to effective transportation of nutrients inside stolons. While in *Bowerbankia* the cincture cells show thick and thin filaments whose diameters resemble those of myofilaments (Gordon, 1975), the present study did not reveal f-actin in the equivalent cells of *H. expansa*. F-actin signal is present in the special cells, however, and they project through the pore medially to the cincture cells.

Autozooidal functional morphology

The autozooids confirm the general morphology as previously reported (Ehlers, 1876). They are vase shaped, translucent and possess noncalcified chitinous cystids (Ehlers, 1876, Mukai et al., 1997). The two space balloons are positioned fronto-laterally on the distal part of the autozooids (Ehlers, 1876; mentioned as "horns"). Apart from the cellular lining the spheres are filled with fluid. Since this thin cellular lining on the inner side of the space balloons cystid wall is still present in adult autozooids, a connection to the rest of the body fluid would be necessary to nourish this cell layer. Previous reports of perforations that connect the fluids of the body cavity and those of the space balloons (Joyeux-Laffuie, 1888) were not observed in the present study. Hence it is assumed, that this cell lining is an ontogenetic rudiment which should eventually dissolve once the nutrient reservoir is exhausted. The space balloons themselves are regarded as buds that did not fully develop into autozooids (Joyeux-Laffuie, 1888), and the position also resembles the budding area (disto-lateral) of other gymnolaemates (Jebram, 1986). Regarding the

environment of *H. expansa*, it can be assumed that multiple tube layers secreted by the polychaete worm increase the pressure on the autozooids and the colony. *H. expansa* is obviously adapted to the mechanical pressure created by the movement of the annelid inside its tube. The lophophore retraction and protrusion processes must be maintained in this environment (Joyeux-Laffuie, 1888). Classical studies reported that an increasing mechanical pressure to the cystid walls lead to the inability of retraction (Joyeux-Laffuie, 1888). The previous hypothesis, that the space balloons provide enough space for the rest of the autozooids between the layers of the polychaete tube to maintain their natural shape and ability to protrude and retract the lophophore, thus appears sound (Joyeux-Laffuie, 1888).

Autozooid musculature

Parietal muscles and retractor muscles

Parietal muscles and retractor muscles play a crucial role in retraction and protrusion of the polypide. The former are an apomorphy of Gymnolaemata and consist of paired consistent rows of transversal muscles (Mukai et al., 1997). They are the major effectors in protrusion of the polypide out of the cystid; when contracted, the cystid wall is bent inwards and increases the pressure in the body cavity which leads to protrusion of the polypide. While usually symmetric in Gymnolaemata, several laterally and often asymmetrically situated parietal muscle bundles in *Hislopia malayensis* are present (Schwaha et al., 2011). The strategy of eversion of the lophophore exists in different versions among bryozoans (Taylor, 1981; Mukai et al., 1997). Phylactolaemates possess a regular grid of body wall musculature that consists of two layers: (i) the outer layer of circular musculature and (ii) an inner layer of longitudinal musculature (Mukai et al., 1997, Gruhl et al., 2009). In cyclostomes, a series of annular muscles are present inside their membranous sac (Nielsen and Pedersen, 1979; Mukai et al., 1997).

The smooth retractor muscles are the most prominent muscles in bryozoans and occur in two bundles that originate from the cystid wall proximally or laterally, travel distally and insert into the lophophoral base (Mukai et al., 1997). Their purpose lies in a quick retraction of the lophophore in all known bryozoans. This condition is also present in *Hypophorella expansa* (Ehlers, 1876).

Tentacle sheath musculature in Bryozoa

The tentacle sheath surrounds the tentacles when the polypide is retracted (Mukai et al., 1997). Longitudinal muscles are present inside the tentacle sheath in phylactolaemates. An orthogonal net-like arrangement consisting of both longitudinal and circular tentacle sheath myofibrils was only recently described for two phylactolaemates (Gawin et al., 2017). In Gymnolaemata and Cyclostomata only regular longitudinal myofibrils of the tentacle sheath are present and range from the distal diaphragm to the lophophoral base (Mukai et al., 1997). The tentacle sheath musculature of *H. expansa* possesses diagonal myofibrils which originate at the lophophoral base, project distally and create a helicoidal net-like muscular basket. Distally, these myofibrils extend into four distinct muscle bundles, the parieto-vaginal bands. Two are located each on the latero-frontal and on the basal side. The former extend from the latero-frontal side of the tentacle sheath to the base of the fronto-lateral space ballons and the latter extend from the latero-basal side of the tentacle sheath to the basal side of the distal diaphragm. Phylactolaemata, widely accepted as the sister group to all remaining Bryozoa, also possess muscle bundles inside the homologous duplicature bands (Schwaha et al., 2011). The arrangement of the tentacle sheath myofibrils in *H. expansa* differs strongly compared to other gymnolaemates and indicates a possible modification due to the unique life style and habitat. A recent study shows that all investigated species of Walkerioidea possess a similar muscle arrangement of the tentacle sheath (Schwaha, submitted). The successive reduction and the more efficient use of less musculature in the evolution of Bryozoa (Phylactolaemata with prominent body wall musculature,

Gymnolaemata with in relation to Phylactolaemata less elaborated parietal muscles and Stenolaemata with annular musculature of the membranous sac) may also be present in case of tentacle sheath musculature. An orthogonal net of both longitudinal and circular tentacle sheath musculature in Phylactolaemata probably grants more stability but is also costly to maintain. The helicoidally arranged net of tentacle sheath musculature in Walkerioidea consisting only of longitudinal muscle fibers may therefore be as stabilizing as an orthogonal muscular net but without the higher costs of additional circular musculature.

Tentacle and digestive tract musculature

The tentacles in *Hypophorella expansa* contain two longitudinal muscle strands, although none were observed in the original description (Ehlers, 1876). This feature is found in all bryozoans. Striated tentacle myofibils are present in ctenostomes (Smith, 1973; Mukai et al. 1997; Schwaha et al., 2011), cyclostomes (Borg, 1926) and two phylactolaemates (Gawin et al. 2017), while cheilostomes possess smooth ones (Gordon, 1974; Schwaha et al. 2011). The observation of striated tentacle muscles in *H. expansa* coincides with previous observations on ctenostomes. This indicates that the last common ancestor of Bryozoa also possessed two striated longitudinal tentacle muscles and inside Bryozoa the presence of smooth tentacle myofibrils is an apomorphy of cheilostomes. *H. expansa* possesses actin concentrations at their distal tentacle areas. Such a condition was only reported recently for the ctenostome *Hislopia malayensis* (Schwaha et al., 2011). Sperm release through the tips of either the two anal-most tentacles in the cheilostome taxon Membraniporoidea or the tips of all tentacles in all other investigated cheilostomes has previously been reported (Silén, 1966, 1972). It is assumed that the actin signal represents a delicate muscular sphincter that facilitates closure of the tentacle coelom. Since *H. expansa* possesses distal muscular tips in each tentacle, it is assumed, that sperm release is conducted through all tentacles. Circular basal transverse muscles are present in *H. expansa*. The ctenostome *H. malayensis* lacks distinct basal transverse muscles but a ring muscle situated at

the lophophoral base may constitute a homologous structure (Schwaha et al., 2011). Circular basal transverse muscles were also reported for the cheilostome *Cryptosula pallasiana* (Gordon, 1974). This indicates that the distinct ring muscle (*H. malayensis*) and the short transverse muscles (*H. expansa* and *C. pallasiana*) are homologous. This scenario is further supported by a recent phylogenetic analysis in which cheilostomes are more closely related with Hislopioidea (Todd, 2000). This indicates that the homologous ring muscle of *H. malayensis* has evolved in the last common ancestor of Hislopioidea and that more derived ctenostomes (such as *H. expansa*) and cheilostomes (such as *C. pallasiana)* still possess the homologous basal transversal muscles. Buccal dilatators are known in cheilostomes (Calvet, 1900), ctenostomes (Brien, 1960; Schwaha et al. 2011) and several cyclostomes (Borg, 1926; Nielsen, 1970). *Hislopia malayensis* possesses two pairs of buccal dilators at the site where the cerebral ganglion is positioned, with one inserting more proximally and the other one more distally to the pharynx (Schwaha et al. 2011). The presence of V-shaped muscular ramifications proximal to the tentacle muscle strands as in *H. expansa* was only reported once in *H. malayensis* (Schwaha et al., 2011). They may play a role in lophophore movement (Schwaha et al., 2011). Striated circular musculature of the pharynx is considered as a common trait among all bryozoans. It is also present in *H. expansa*, where it builds a myoepithelium as in all other ctenostomes (Henneguy, 1909; Braem, 1940; Brien, 1960; Bullivant, 1968; Matricon, 1973) and few cheilostomes (Henneguy, 1909; Renieri, 1970; Gordon, 1975). Therefore, a myoepithelium seems to be part of the ground pattern in Gymnolaemata. The pharynx and esophagus of *H. expansa* consists of both striated longitudinal and circular myofibrils. Cardia and caecum possess smooth ones and the intestine only longitudinal musculature. Additional pharyngeal longitudinal myofibrils are present in the ctenostome *Bowerbankia pustulosa* (Schwaha et al., 2011) and for the phylactolaemate *Asajirella gelatinosa* (Mukai et al., 1997). An outer layer of few striated longitudinal muscles was reported in the pharynx of cyclostomes (Borg, 1926). A pharynx only supplied with circular musculature is sometimes considered an ancestral condition of Phylactolaemata (Gawin et al.,

2017). However, the presence of additional longitudinal myofibrils in the pharynx of the phylactolaemate *Asajirella gelatinosa*, in ctenostomes and cyclostomes indicates that such myofibrils represent an ancestral trait in Bryozoa in general. Otherwise it evolved multiple times independently, once in Phylactolaemata and at least once in Ctenostomata and Cyclostomata. From a parsimonious point of view, the first hypothesis would be more probable in which it was present in the last common ancestor of Bryozoa and reduced once in Phylactolaemata.

Defining the transition from the pharynx to the esophagus is challenging in many bryozoans. The pharyngeal-esophageal border may often not be a sharp one and is mostly only resolvable by comparing the ciliation pattern (Silén, 1944). In case of *H. expansa* the ciliation of the pharynx is limited to its distal bulbous region, which would indicate the beginning of the esophagus proximally to it, at the point where the ciliation ceases. The cardia shows ciliation after the cardiac valve. A more delicate but very consistent ciliation of the caecum and a very dense and prominent one of the pylorus and intestine is present. The cardia may be differentiated into a gizzard or proventriculus in some ctenostomes. Vesicularioideans often possess a bulbous gizzard that is said to crush food particles (Jebram, 1973; Schwaha et al., 2011). A gizzard is not present in *H. expansa*, which coincides with the reports that such a gizzard is absent in most other major ctenostome clades such as the Walkerioidea, Victorelloidea, Alcyonidioidea and Arachnidioidea (Jebram, 1973). The transition from the cardia to the caecum in ctenostomes is marked by a muscular sphincter at the end of the cardia adjacent to the caecum (Jebram, 1973). This cardia sphincter is homologous to the gizzard (Jebram, 1973) and is generally present in Victorelloidea (Braem, 1951; Markham & Ryland, 1987) and also in many Walkerioidea such as *H. expansa* (this study). The caecal musculature of *H. expansa* mainly consists of regular loose smooth circular and fewer, more irregular, smooth longitudinal muscle fibers. The caecum of *Hislopia malayensis* consists of prominent circular and few sparse and short longitudinal muscle fibers. Two additional prominent longitudinal muscles at the proximal side of the caecum were reported (Schwaha et al., 2011). These are not present in *H. expansa*. The caeca in *Flustrellidra*

hispida (Graupner, 1930) and in *Amathia (Zoobotryon) verticillata* (Gerwerzhagen, 1913) possess rather short longitudinal muscle fibers in their lateral parts (termed plasmodesmata), whereas in *H. expansa* delicate but distinct longitudinal muscle fibers are present. In conclusion it seems that early branches in ctenostomes possess sparse and short caecal longitudinal muscle fibers and these elongated and became distinct in later branches such as Walkerioidea.

The intestine of *H. expansa* consists of several delicate smooth longitudinal muscles. Similar situations were reported for the alcyonioid ctenostomes *Alcyonidium mytili* (Silbermann, 1908) and *A. variegatum* (d'Hondt and Gusso, 2006), the ctenostomes *Harmeriella terebrans* (Borg, 1940) and *Hislopia malayensis* (Schwaha et al., 2011) and cyclostomes (Schwaha et al., 2018, submitted). An intestine solely with longitudinal musculature seems to be a common trait among Gymnolaemata and Stenolaemata in general. Since phylactolaemates possess intestinal ring musculature and no longitudinal myofibrils (Mukai et al., 1997) and Gymnolaemata and Cyclostomata only possess longitudinal myofibrils, the last common ancestor of Stenolaemata and Gymnolaemata may have also possessed only longitudinal intestinal myofibrils.

A distal anal position as found in *Hypophorella expansa* was is also present in several alcyonidioids (Silbermann, 1908; Ryland and Porter, 2006) and *Harmeriella terebrans* (Borg, 1940). The anus is positioned more or less on the proximal half of the tentacle sheath in the vesicularioid *Amathia verticillata* (as *Zoobotryon pellucidum*, Gerwerzhagen, 1913), the alcyonidioid *Flustrellidra hispida* (as *Flustra hispida*, Graupner, 1930), the hislopioid *Hislopia malayensis* (Schwaha et al., 2011) and the paludicellioid *Paludicella articulata* (Weber et al. 2014; Schwaha and Wanninger, 2015). From a parsimonious perspective it seems that a proximally positioned anus reflects the ground pattern in ctenostomes whereas the distal condition probably evolved at least twice independently (at least once in Alcyonidioidea and once in Walkerioidea).

Apertural musculature and movement of the gnawing apparatus in *Hypophorella expansa*

The vestibulum is an invagination of the distal cystid wall. In all bryozoans the distal end of the tentacle sheath is separated from the vestibular wall by a diaphragm which possesses a diaphragmatic sphincter (Mukai, 1997; Schwaha at al., 2011). Vestibulum, diaphragm and distal tentacle sheath are associated with apertural musculature in *Hypophorella expansa*. In general, gymnolaemates possess two apertural muscular systems. The first are the "parieto-vaginal bands" that are homologues of the phylactolaemate "duplicature bands" in cheilo- and ctenostomes (Schwaha et al., 2011). The second are prominent vestibular muscles (Schwaha et al., 2011). The attachment organ in cyclostomes connects the membranous sac to the zooid walls (Mukai et al., 1997). This attachment organ is topologically similarly positioned as are the duplicature bands in phylactolaemates (Schwaha et al., 2011). The parieto-vaginal bands of ctenostomes are reduced in Hislopioidea, Victorelloidea, Vesicularioidea and nearly all Walkerioidea, but present in Alcyonidioidea and Paludicelloidea (Schwaha et al., 2011). *H. expansa* is the only walkerioid for which four distinct parieto-vaginal bands were reported (Ehlers, 1876; this study). For *Farrella repens* parieto-vaginal bands were indicated, but not specifically mentioned (as *Laguncula repens*; van Beneden, 1845). Since duplicature bands are present in phylactolaemates and their homologues, the parietovaginal bands in early branches of ctenostomes, this indicates that these parietovaginal bands are part of the ctenostome ground pattern and were reduced several times during ctenostome evolution.

In *Hypophorella expansa*, the vestibulum possesses a prominent, dense arrangement of ring muscles, the vestibular wall muscles embedded in the vestibular epithelium. They are associated with several longitudinal muscle bundles. Two distinct short muscle bundles originate on the lateral side of the vestibular ring muscles and insert medially at the gnawing apparatus which lies on the basal part of the vestibulum. The relative position of tentacle sheath, diaphragmatic sphincter and vestibular wall musculature in *H. expansa* is different when the lophophore is protruded and retracted. The protrusion and gnawing process was previously described, although

limited to light microscopy studies (Ehlers, 1876, Prouho, 1892). The new data collected during this work allows a more accurate description of the position of certain muscle groups when the lophophore is retracted and protruded. During the polypide protrusion the lophophore passes first the tentacle sheath, followed by the diaphragmatic sphincter and lastly the vestibular wall. When the lophophore is protruded, tentacle sheath, diaphragmatic sphincter and vestibulum are aligned linearly and unfolded. This is not the case while the lophophore is retracted because the diaphragmatic sphincter is positioned basally of the vestibulum. This way the aperture musculature would be efficiently placed inside the cystid which has limited space. During the eversion process the arrangement of these muscular systems passively follows the protrusion of the polypide and obtains a linear alignment. Since the gnawing apparatus is embedded in the vestibular wall, it is also moved during these processes. There was no musculature observed during this study that would indicate an ability of autonomous movement of the gnawing apparatus.

Previous studies investigated the apertural musculature associated with the gnawing apparatus of *H. expansa* (Prouho, 1892). The illustrated muscle bundles in this previous study are somewhat misleading, as they could indicate that the gnawing apparatus possesses two (or three) distinct muscle bundles that could directly move the gnawing apparatus, regardless of polypide eversion or retraction (Fig. 4 D-F; Prouho, 1892). The first insert at the middle length of the gnawing apparatus' proximal base, interconnecting the separated teeth rows (Prouho, 1892; Fig. 4 D, E, marked as m^3). The second inserts at the lateral-most ends of these two gnawing rows (Prouho, 1892; Fig. 4 D-F, marked as m^4). Compared to the results of this work, m^3 would represent the two vestibular muscle bundles that connect to the gnawing apparatus (Fig. 4 D, E; Fig. 7 C). The muscle bundles m^4 are the circular musculature of the vestibular wall to which the muscles associated with the gnawing apparatus (Prouho, 1892; Fig. 4 D-F, marked as m^4) are connected. These two muscle bundles were previously interpreted as one single muscle bundle (Prouho, 1892; Fig. 4 D). The arrangement of the two teeth-bearing rows of the gnawing apparatus

probably occurs while passively following the movement of the vestibular wall after the contraction of the parietal muscles, changing from an "M"-like shape to a "C"-shape (Fig. 4 A, B, C). The contraction of the retractor muscles leads to a quick retraction of the lophophore (Mukai et al., 1997). At the end of the retraction process, the vestibular muscle bundles connected to the gnawing apparatus probably move the medially adjacent parts of the teeth rows towards their concave sides. Additionally, the aperture musculature would contract to position the diaphragmatic sphincter basally to the vestibular wall musculature. The latter should also, due to muscle contraction, get into the observed state while the lophophore is retracted (as was shown in this work). The two muscle bundles that connect to the gnawing apparatus may be vestibular wall ring muscles which gained a new function in this species compared to its ancestor and could be regarded as vestibular wall muscle homologs (homology criterium of position). The "stoloniferan" ctenostome *Harmeriella terebrans* exhibits a similar boring life style as *Hypophorella expansa as* it inhabits the calcareous cystids of cheilostomes (Borg, 1940). This species was observed only once and it also belongs to the Walkeroidea (Borg, 1940). Similar to *H. expansa*, its vestibular wall possesses (probably chitinous) tooth-like structures on the surface of its epidermis that provide the function of a gnawing apparatus (Borg, 1940).

Nervous system

Cerebral ganglion in Bryozoa

With its crucial involvement in feeding and as the site of the central nervous system (cerebral ganglion) the lophophoral base is considered the most complex part of a polypide (Mukai et al., 1997). Despite the importance of the nervous system, studies and data gained from immunocytochemical methods and confocal laser scanning microscopy are still scarce (Weber et al., 2014; Shunkina et al., 2015; Temereva and Kosevich, 2016; Ambros et al., 2018). Previous

reports on the position and shape of the cerebral ganglion of *Hypophorella expansa* coincide with the observed situation in this work. It is an ovally to quadrangularly shaped organ and is positioned at the anal side of the lophophoral base (Ehlers, 1876). This also reflects the common position of the central nervous system in ctenostomes and Bryozoa in general (Lutaud, 1977, Mukai et al., 1997).

Tentacle sheath innervation in Bryozoa

The tentacle sheath innervation in the phylactolaemates *Cristatella mucedo*, *Plumatella repens* and *Fredericella sultana* emerges from the basal radial nerves of the cerebral ganglion and further forms a nerve plexus (Gerwerzhagen, 1913; Shunkina et al., 2015). For the phylactolaemate *Hyalinella punctata* neurite bundles were reported that originate at several sites at the lophophoral base to innervate the tentacle sheath with a nerve plexus over its whole range (Ambros et al., 2018). Two distinct neurite bundles that emerge from the cerebral ganglion to innervate the tentacle sheath are present in the ctenostome *Amathia gracilis* (Temereva and Kosevich, 2016). A similar situation is present in the ctenostome *Flustrellidra hispida* where the two tentacle sheath nerves fuse distally (Graupner, 1930). In the cheilostome *Electra pilosa* two short tentacle sheath neurite bundles emerge from the cerebral ganglion laterally and bifurcate after a short distance to give rise to four tentacle sheath neurite bundles (Lutaud, 1977). The neurite bundle closer to the median axis on the anal side distally to the ganglion is termed the "direct nerve" (Lutaud, 1977); the lateral "trifid nerve" (a three-branched strand of which the first two innervate the gut and the retractor muscles; the third branch bends distally from the pharynx and progresses along the tentacle sheath, and joins the direct nerve (Lutaud, 1977). The direct and trifid nerves fuse and give rise to the "great tentacle sheath nerve" (Lutaud, 1977). This neurite bundle possesses a circular branch more distally that partially encircles the tentacle sheath (Lutaud, 1977). The trifid nerve of *Flustrellidra hispida* ramifies twice with a first branch forming a tentacle sheath ring nerve proximally of the fusion of the trifid and direct neurite

bundles. The second ramification occurs more distally after the fusion of trifid and direct nerve and gives rise to circular branches that progress laterally on the oral and anal side (Graupner, 1930). Similar circular branches are present in *Hypophorella expansa* (this study). Two pairs of neurite bundles originate from the cerebral ganglion, the inner "direct nerves" and the lateral "trifid nerves" (sensu Lutaud, 1977). The distally branching part of the "trifid nerve" fuses with the circular branch of the "direct nerve" on the anal side and continues distally along the entire tentacle sheath. These data indicate that gymnolaemates in general have only few tentacle sheath neurite bundles on the anal side of the polypide, whereas phylactolaemates have a diffuse plexus with only few indications of thicker neurite bundles on the anal and oral side.

Tentacle innervation in Bryozoa

The reported tentacle innervation pattern for Gymnolaemata with one abfrontal, one medio-frontal and one pair of latero-frontal neurite bundles (Gruhl and Schwaha, 2015) is also present in *Hypophorella expansa*. All mentioned tentacle neurite bundles are located basiepithelially. A recent study of the ctenostome *Paludicella articulata* showed the same condition (Weber et al., 2014). In the cheilostome *Cryptosula pallasiana* two additional lateral subperitoneal tentacle neurite bundles were found (Gordon, 1974) whereas the abfrontal, medio-frontal and latero-frontal neurite bundles project basiepithelially. In gymnolaemates, medio-frontal and abfrontal neurite bundles innervate the frontal/abfrontal tentacle muscles, respectively (Mukai et al. 1997). In *H. expansa* both the frontal/latero-frontal tentacle neurite bundles and the abfrontal tentacle neurite bundle lie basiepithelially. In ctenostomes the mediofrontal neurite bundles arise from the cerebral ganglion (anal side) or the circum-oral nerve ring (oral side) in the median axis of each tentacle, whereas in cheilostomes both the frontal and abfrontal neurite bundles have a similar origin (Bronstein, 1937; Schwaha and Wood, 2011; Weber et al. 2014; Gruhl and Schwaha, 2015; Temereva and Kosevich, 2016). In *H. expansa* a different situation is present, in which all tentacle neurite bundles originate from intertentacular forks on both the anal and the oral side. A

different innervation pattern between tentacles of the oral and anal side, as is present in *H. expansa* (this work) and also in the ctenostome *Amathia gracilis* (Temereva and Kosevich, 2016). In these two species the abfrontal tentacle neurite bundle on the oral side arises as a single bundle from an intertentacular fork and only innervates the adjacent tentacle closer to the oral-most side (Temereva and Kosevich, 2016; this study). Intertentacular forks on the anal side in *A. gracilis* innervate two neighboring tentacles with abfrontal tentacle neurite bundles such as found in *H. expansa* (Temereva and Kosevich, 2016; this study). A small difference is present in *H. expansa*, however. On the anal side the anal-most tentacle is only innervated by an abfrontal neurite bundle of one intertentacular fork, which was not reported for *A. gracilis* (Temereva and Kosevich, 2016). The tentacle innervation of *Farella repens* consists of two median neurite bundles directly arising from the circumoral nerve ring basally to the median axis of a distal tentacle (Bronstein, 1937). Additionally, the laterofrontal tentacle neurite bundles originate from intertentacular forks, which innervate two neighboring tentacles (Bronstein, 1937). The only ultrastructural studies are on *Crisia eburnea*, which posseses one mediofrontal and abfrontal and two laterofrontal tentacle neurite bundles (Nielsen and Riisgard, 1998). The branching from the lophophoral base, however, has not been described.

Recent studies reported six subepidermal tentacle neurite bundles for the phylactolaemates *Cristatella mucedo*, *Plumatella repens*, *Fredericella sultana* and *Hyalinella punctata* (Shunkina et al., 2015; Ambros et al., 2018). These species possess two laterofrontal and one median tentacle neurite bundle on both the frontal and abfrontal side (Shunkina et al., 2015; Ambros et al., 2018). They arise from intertentacular radial neurite bundles which innervate two neighboring tentacles each. *H. punctata* differs slightly from this condition in that, the abfrontal tentacle neurite bundle arises from the two latero-abfrontal tentacle neurite bundles that branch and fuse distally of the tentacle base to form the abfrontal tentacle neurite bundle (Ambros et al., 2018). The tentacles of *Lophopus crystallinus* are innervated by six tentacle neurite bundles; two laterofrontal and abfrontal, one mediofrontal and one abfrontal tentacle neurite bundle (Gruhl

unpublished data, cited in Shunkina et al., 2015). Lophopodidae is considered to be part of an early branch in Phylactolaemata (Hirose et al., 2008). *Asajirella gelatinosa* also belongs to the Lophopodidae and possesses up to 10 tentacle neurite bundles, but the level of the cross section was not defined (Mukai et al., 1997). It is possible that more distal cross sections show a different picture if some of these reported neurite bundles merge further distally (Mukai et al., 1997). Based on the recent phylogenetic analysis of Phylactolaemata it is hereby assumed that the phylactolaemate ancestor possessed six tentacle neurite bundles of an intertentacular origin (Hirose et al., 2008). The unpublished data from Gruhl (Shunkina et al., 2015) and the reported tentacle innervation of *Hislopia malayensis* (Schwaha and Wood, 2011) indicate that the last common ancestor of Gymnolaemata and Stenolaemata exhibited four tentacle neurite bundles of which the mediofrontal neurite bundle arises directly from the circumoral nerve ring. Since the cheilostome *Cryptosula pallasiana* possesses the same amount of tentacle neurite bundles as phylactolaemates (six) with two of them being subperitoneal (Gordon, 1974; Phylactolaemata only possess subepithelial ones) it is concluded that these two subperitoneal neurite bundles are not homologous to the phylactolaemate latero-abfrontal neurite bundles and have evolved independently in cheilostomes. The innervation pattern of *H. expansa* (Walkerioidea) with all neurite bundles emerging from intertentacular forks indicates that it has evolved secondarily in this species, since the tentacle innervation of *Farella repens* (Walkerioidea) resembles that of earlier branches in ctenostomes, with the abfrontal tentacle neurite bundle arising directly from the circumoral nerve ring (Bronstein, 1937).

Visceral innervation in Bryozoa

The innervation of the foregut arises from the cerebral ganglion. One main medio-visceral neurite bundles, two to five medio-lateral visceral neurite bundles and two latero-visceral neurite bundles are present in *Paludicella articulata* (Weber et al., 2014). *Amathia gracilis* possesses one medio-visceral neurite bundle, two medio-lateral visceral neurite bundles and two latero-

visceral neurite bundles (Temereva and Kosevich, 2016). *Hypophorella expansa* (this study) exhibits the same condition as *A. gracilis* even though the latero-visceral neurite bundles of *A. gracilis* were not explicitly mentioned but only indicated as part of the circum-pharyngeal nerve plexus (Temereva and Kosevich, 2016). Cheilostomes possess a similar innervation pattern, with one medio, two medio-lateral and two latero-visceral neurite bundles (Lutaud, 1993). A diffuse nerve plexus with two more prominent medio-lateral neurite bundles which emanate from the cerebral ganglion proximally and innervate the foregut are present in phylactolaemates (Shunkina et al., 2015; Ambros et al., 2018).

The visceral innervation proceeds towards the cardiac valve in *H. expansa* (this work). This coincides with previous reports for phylactolaemates and one cheilostome which possess a distinct innervation of the cardiac valve forming a nerve ring (Gerwerzhagen, 1913; Schwaha and Wanninger, 2015). The latter study was conducted using serotonin antibodies and it was concluded that serotinin is probably deployed as a neurotransmitter in sensory transduction in Bryozoa (Schwaha and Wanninger, 2015). The visceral innervation of the ctenostome *Paludicella articulata* also proceeds proximally until the cardiac valve (Schwaha and Wanninger, 2015). These data imply a transition from a diffuse nerve plexus in Phylactolaemata towards few distinct visceral neurite bundles in Gymnolaemata that innervate the foregut. Since medio-lateral neurite bundles innervating the foregut are also present in Phylactolaemata the medio-lateral visceral neurite bundles of gymnolaemates may be homologs to the longitudinal neurite bundles in phylactolaemates. This implies that at least the last ancestor of Gymnolaemata probably possessed a distinct medio-visceral neurite bundle since such a neurite bundle is present in early branches of Ctenostomata. Whether this was also the case for the last common ancestor of Gymnolaemata and Stenolaemata remains speculative since data on the nervous system of cyclostomes are still lacking.

Apertural and parietal innervation in Gymnolaemata

The apertural innervation in *Hypophorella expansa* has its origin in the compound tentacle sheath neurite bundles (i.e. great tentacle sheath nerve, sensu Lutaud), which project distally to the apertural area. This coincides with the reports for *Flustrellidra hispida.* This species also possesses an apertural nerve ring proximal to the orifice (Graupner, 1930). Such a nerve ring however, is not present in *H. expansa*. The compound tentacle sheath neurite bundles of the cheilostome *Electra pilosa* innervate the diaphragm, the operculum occlusors and the parietal muscles (Lutaud, 1977). In *E. pilosa*, this compound neurite bundle splits distally into three minor neurite bundles with one innervating the diaphgram with its sphincter muscle. The second one innervates the operculum occlusors. The third neurite bundle projects towards the frontal wall to innervate the parietal muscles (Lutaud, 1977). *H. expansa* does not possess an operculum but shares the remaining innervation pattern of the aperture and the parietal muscles with *E. pilosa*. The compound tentacle sheath nerve (fused direct and distal branch of the trifid neurite bundle) of *H. expansa* innervates the tentacle sheath and extends to the apertural area. Proximally of the apertural area, a parietal neurite bundle branches laterally and projects along the parieto-vaginal bands towards the frontal body wall at the base of the space balloons. The neurite bundle then bends proximally and innervates the parietal muscles in a meandering way. This also resembles the reported parietal innervation of the ctenostome *Paludicella articulata* (Schwaha and Wanninger, 2015). The innervation patterns of the aperture and the parietal muscles as described above show strong similarities and may thus be part of the ground pattern of Gymnolaemata.

Conclusion and outlook

The following morphological apomorphies can be ascertained for *Hypophorella expansa*. Space balloons on the fronto-lateral side of the autozooids provide space between successively secreted tube layers of the polychaete host. The stolons possess a median transversal muscle in their distal capsules and a peculiar wrinkling at the inner surface of their ectocysts proximally to them. The wrinkles project inside the stolon lumen and may provide mechanical stability regarding the thinness of the stolons but may also enhance circulation of body fluid via the transverse muscle in the capsule (see also Jebram, 1973). The growth pattern of *H. expansa* may be an efficient way to colonize the space in between the layers of the polychaete tube. Since only one lateral autozooid is attached on a distal stolon capsule, the successive distal and lateral stolons allow for a fast, two-dimensional dispersal of the colony. Autozooids of *H. expansa* possess a mechanical gnawing apparatus which is integrated into their vestibular walls and is associated with the apertural musculature. The gnawing procedure is probably linked to the protrusion mechanism of the polypide, since it is devoid of any musculature that could lead to the conclusion that the apparatus could perform autonomous movements. Interestingly, a similar association of gnawing structures and the vestibular epidermis are present in the "stoloniferan" ctenostome *Harmeriella terebrans*, which bores on calcified cheilostome cystid walls. These two species are part of Walkerioidea since both *H. expansa* and *H. terebrans* possess stolons and lack a gizzard. Unfortunately, the latter has never been re-encountered after its discovery, as had been *H. expansa* for a long period of time. A re-investigation and comparison of boring bryozoan in general using state-of-the-art methods are vital to assess morphological adaptations related to their boring life-style.

Acknowledgements

Literature

Ambros M, Wanninger A, Schwaha TF. 2018. Neuroanatomy of *Hyalinella punctata*: Common patterns and new characters in phylactolaemate bryozoans. Journal of Morphology. 00:1-17.

Borg F. 1926. Studies on recent cyclostomatous Bryozoa. *Zool Bidr Uppsala*. 10:181-507.

Borg F. 1940. On the genus *Tubiporella* and on a new boring Bryozoan. *Zool. Bidr. Uppsala*. 415-439.

Braem F. 1940. Über die Querstreifung im Pharynx der gymnolämen Bryozoen und über den Bau des Munddarms. *Z Morph Ökol Tiere*. 36:688-676.

Braem F. 1951. Über *Victorella* und einige ihrer nächsten Verwandten, sowie über die Bryozoenfauna des Ryck bei Greifswald. *Zoologica*. 102:1-59.

Brien P. 1960. Classe des Bryozoaires. In: *Traite de Zoologie. Anatomie, Systématique, Biologie*. Edited by Grassé PP. Paris: Masson. 5:1053-1335.

Bronstein G. 1937. Étude du système nerveux de quelques bryozoaires gymnolémides. *Trav. Stat. Biol.* Roscoff. 154-174.

Bullivant JS, Bils RF. 1968. The pharyngeal cells of *Zoobotryon verticillatum* (delle Chiaje), a gymnolaemate bryozoan. *NZ J Mar Freshw Res* 2:438-446.

Calvet L. 1900. Contribution à l'histoire naturelle des Bryozaires Ectoproctes marins. *Travaux de l'institute de zoologie de Montpellier*. 8:1-488.

D'Hondt J-L, Chimenz Gusso C. 2006. Note sur quelques bryozoaires cténostomes des côtes italiennes et turques. *Bull. Soc. Zool. Fr.* 131(2):107-116.

Ehlers E. 1876. *Hypophorella expansa*, ein Beitrag zur Kenntnis der minierenden Bryozoen. *Abhand Koenigl Gesellsch Wiss Goett*. 21:1-156.

Gawin N, Wanninger A, Schwaha TF. 2017. Reconstructing the muscular ground pattern of phylactolaemate bryozoans: first data from gelatinous representatives. *BMC Evolutionary Biology*. 17:225:1-19.

Gerwerzhagen A. 1913. Untersuchungen an Bryozoen. *Sitzungsberichte der Heidelberger Akademie der Wissenschaften*. Stiftung Heinrich Lanz. Mathematisch-naturwissenschaftliche Klasse. Abteilung B. Biologische Wissenschaften. 9:1-16.

Gordon DP. 1974. Microarchitecture and function of the lophophore in the bryozoan *Cryptosula pallasiana*. In: *Marine Biology*. Springer-Verlag. 27:147-163.

Gordon DP. 1975. Ultrastructure of communication pore areas in two bryozoans. *Docum. Lab. Géol. Fac. Sci. Lyon* - H.S. 3 (fasc. 1). 187-192.

Gordon DP. 1975. Ultrastructure and function of the gut of a marine bryozoan. In: *Cahiers de biologie marine*. Quai Saint-Bernard. Paris-V*. C. C. P. Paris. 14.211-51. 9:367-386.

Graupner H. 1930. Zur Kenntnis der feineren Anatomie der Bryozoen. *Zeitschrift für wissenschaftliche Zoologie*. 135:38-77.

Gruhl A, Schwaha TF. 2015. Bryozoa (Ectoprocta). In: *Structure and Evolution of Invertebrate Nervous Systems*. Oxford University Press. Great Clarendon Street, Oxford OX2 6DP, UK. 26:325-340.

Gruhl A, Wegener I, Bartolomaeus T. 2009. Ultrastructure of the body cavities in Phylactolaemata (Bryozoa). *Journal of Morphology*. 270(3):306–318.

Henneguy MF. 1909. Sur un épithélium à fibres musculaires striées. *C. R. Hebd. Seances. Académy des sciences*. 148:134-138.

Hayward PJ. 1985. Ctenostome Bryozoans. In: *Synopsis of the British Fauna (New Series)*. Edited by: Kermack DM. Barnes RSK: London etc.: E.J.Brill/Dr.W. Backhuys for The Linnean Society of London. 33:1-169.

Hirose M, Dick MH, Mawatari SF. 2008. Molecular phylogenetic analysis of phylactolaemate bryozoans based on mitochondrial gene sequences. In: S. J. Hageman, M. M. J. Key, & J. E. Winston (Eds.), *Proceedings of the 14th International Bryozoology Association Conference, Boone, North Carolina, Virginia Museum of Natural History Special Publication*. Martinsville, Virginia: Virginia Museum of Natural History. 15:65-74.

Jebram D. 1973. Stolonen-Entwicklung und Systematik bei den Bryozoa Ctenostomata. *Z. zool. Syst. Evolut.-forsch*. 11:1-48.

Jebram D. 1986. Arguments concerning the basal evolution of the Bryozoa. *Z. zool. Syst. Evolut.-forsch*. Verlag Paul Parey. Hamburg und Berlin. 24:266-290.

Joyeux-Laffuie J. 1888. Description du *Delagia chaetopteri*, type d'un nouveau genre de bryozoaires. *Arch. Zool. Exp. Gen*. 2(6):135-154.

Limaye A. 2012. Drishti: a volume exploration and presentation tool. *Preceedings*. Volume 8506, Developments in X-Ray Tomography VIII. 85060X.

Lutaud G. 1977. The bryozoan nervous system. In: *Biology of bryozoans*. Edited by Woollacott RM, Zimmer RL. New York: Academic. 377–410.

Lutaud G. 1993. L'innervation sensorielle du lophophore et de la région orale chez les Bryozoaires Cheilostomes. *Annales des Sciences Naturelles, Zoologie*. Paris. 13(14-4):137-146.

Markham JB, Ryland JS. 1987. Function of the gizzard in Bryozoa. *J ExpMar Biol Ecol*. 107:21-37.

Matricon I. 1973. Quelques données ultrastructurales sur un myoépithélium: le pharynx d'un Bryozoaire. *Z Zellf mikr Anat*. 136:569-578.

Mukai H, Terakado K, Reed CG. Bryozoa. 1997. In: *Microscopic anatomy of invertebrates*. Edited by Harrison FW, Woollacott RM. New York, Chichester: Wiley-Liss; 13:45-206.

Nielsen C. 1970. On metamorphosis and ancestrula formation in cyclostomatous bryozoans. *Ophelia*. 7:217-256.

Nielsen C, Pedersen KJ. 1979. Cystid structure and protrusion of the polypide in *Crisia* (Bryozoa, Cyclostomata). *Acta Zool.* 60: 65-88.

Nielsen C, Riisgard HU. 1998. Tentacle structure and filter-feeding in *Crisea eburnea* and other cyclostomatous bryozoans, with a review of upstream-collecting mechanisms. *Marine Ecology Progress Series*. 168:163-186.

Pohowsky RA. 1975. Boring bryozoa. *Docum. Lab.Géol. Fac. Sci. Lyon*. 3(1):255-256.

Pohowsky RA. 1978. The boring ctenostomate bryozoa: Taxonomy and paleobiology based on cavities in calcareous substrata. *Bulletins of American paleontology*. 73(301):5-183.

Prouho H. 1892. Contribution à l'histoire des Bryozaires. *Arch. Zool. Exp. Gen.* 2(10):557-656.

Renieri T. 1970. Submicroscopical features of alimentary canal in Bryozoa. *J Submicr Cytol.* 2: 181-188.

Ryland JS, Porter JS. 2006. The identification, distribution and biology of encrusting species of *Alcyonidium* (Bryozoa: Ctenostomatida) around the coasts of Ireland. *Biology and Environment: Proceedings of the Royal Irish Academy*. Vol. 106B. 1:19-33.

Schindelin J, Arganda-Carreras I, Frise E, Kaynig V, Longair M, Pietzsch T, Preibisch S, Rueden C, Saalfeld S, Schmid B, Tinevez J, White D J, Hartenstein V, Eliceiri K, Tomancak P, Cardona A. 2012. Fiji: an open-source platform for biological-image analysis. *Nature Methods.* 9:676–682.

Silén L. 1944. On the division and movements of the alimentary canal of the Bryozoa. *Ark Zool.* 35A:1-41.

Silén L. 1966. On the fertilization problem in the gymnolaematous Bryozoa. *Ophelia.* 3:113-140.

Silén L. 1972. Fertilization in the Bryozoa. *Ophelia*. 10:27-34.

Shunkina KV, Zaytseva OV, Starunov VV, Ostrovsky AN. 2015. Comparative morphology of the nervous system in three phylactolaemate bryozoans. *Frontiers in Zoology*. 12:28.

Smith LW. 1973. Ultrastructure of the tentacles of *Flustrellidra hispida* (Fabricius). In: *Living and Fossil Bryozoa*. Edited by: Larwood GP. London: Academic Press. 335-342.

Schwaha T, Wood TS, Wanninger A. 2011. Myoanatomy and serotonergic nervous system of the ctenostome Hislopia malayensis: evolutionary trends in bodyplan patterning of ectoprocta. *Frontiers in Zoology*. 8:11:1-27.

Schwaha T, Wood TS. 2011. Organogenesis during budding and lophophoral morphology of Hislopia malayensis Annandale, 1916 (Bryozoa, Ctenostomata). *BMC Developmental Biology*. 11:23:1-14.

Schwaha T, Wanninger A. 2015. The serotonin-lir nervous system of the Bryozoa (Lophotrochozoa): a general pattern in the Gymnolaemata and implication for lophophore evolution of the phylum. BMC Evolutionary Biology. 15:223:1-11.

Taylor PD. 1981. Function morphology and evolutionary significance of differing modes of tentacle eversion in marine bryozoans. *Recent and Fossil Bryozoa.* Larwood GP, Nielsen C, editors. Fredensborg: Olsen & Olsen. 235-247.

Temereva EN, Kosevich IA. 2016. The nervous system of the lophophore in the ctenostome *Amathia gracilis* provides insight into the morphology of ancestral ectoprocts and the monophyly of the lophophorates. *BMC Evolutionary Biology*. 16:181-204.

Todd JA. 2000. The central role of ctenostomes in bryozoan phylogeny. *Proceedings of the 11th International Bryozoology Association Conference*. 104-135.

van Beneden PJ. 1845. Recherches sur l'organisation des Laguncula, et l'histoire naturelle des différents polypes bryozoaires qui habitent la côte d'Ostende. *Nouv Mém Acad Roy Sci Belles-Lett Brux*. 18:3-29.

Weber AV, Wanninger A, Schwaha TF. 2014. The nervous system of *Paludicella articulata* – first evidence of a neuroepithelium in a ctenostome ectoproct. *Frontiers in Zoology*. 11(1):89-99.

Waeschenbach A, Taylor PD, Littlewood DTJ. 2012. A molecular phylogeny of bryozoans. *Molecular Phylogenetics and Evolution*. 62:718-735.

Figure 1
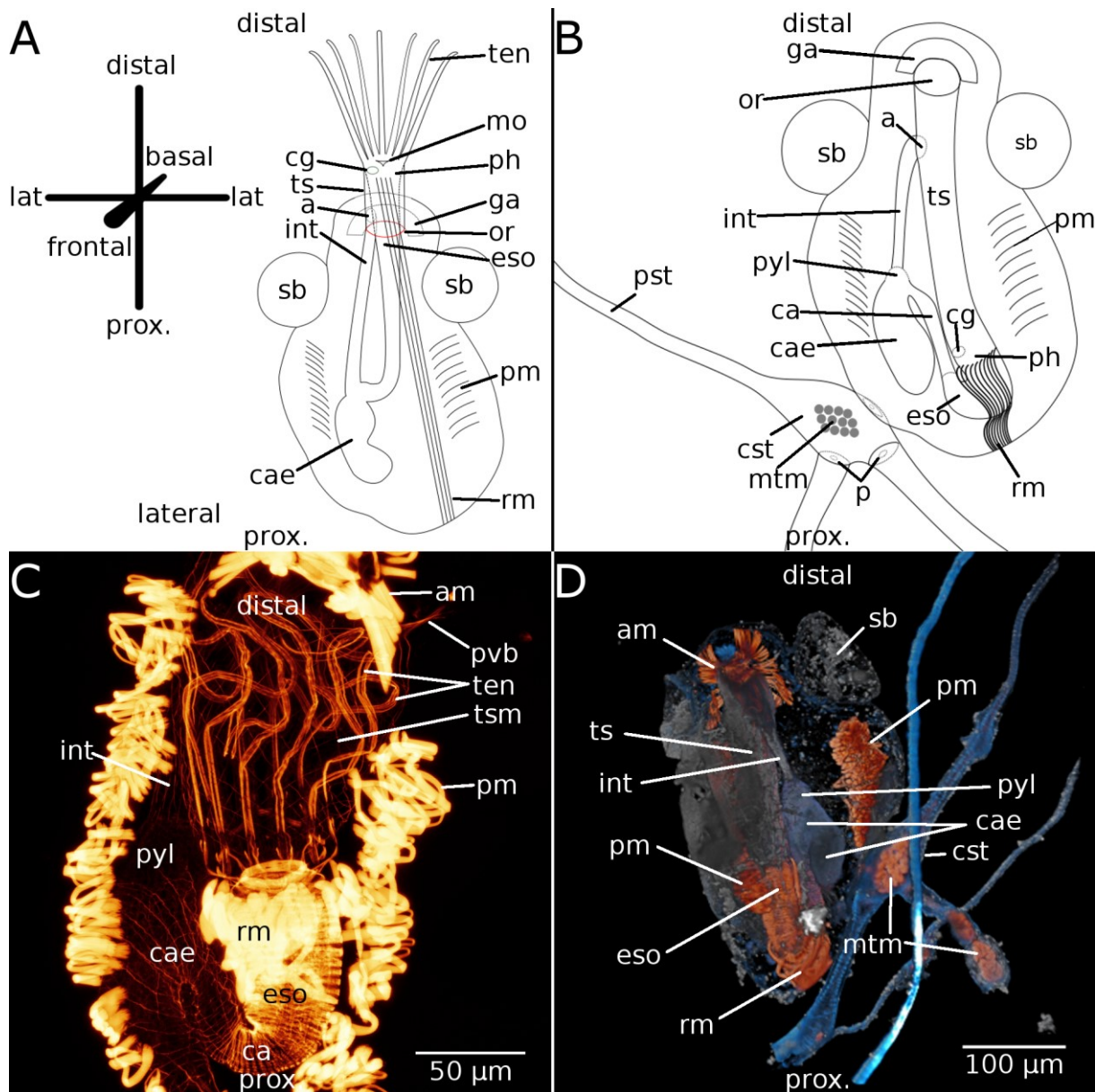
Fig. 1 – Gross morphology of autozooids and stolons of *Hypophorella expansa*. A: Scheme of an autozooid with protruded polypide. Note the scheme on the top left corner that illustrates the spatial orientation of an autozooid. B: Stolon and its corresponding autozooid in retracted state. C: Maximum intensity projection of an autozooid with a retracted polypide. Musculature in orange. D: Volume rendering of an autozooid with its corresponding stolon. Musculature in orange, nuclei in blue and acetylated alpha-tubulin in gray. a – anus, am – aperture musculature, ca – cardia, cae – caecum, cst – stolon capsule, eso – esophagus, ga – gnawing apparatus, int – intestine, mo – mouth opening, mtm – median transversal muscle, or – orifice, p – pore plate, ph – pharynx, pm – parietal muscles, pst – proximal stolon part, pvb – parieto-vaginal bands, pyl –

pylorus, rm – rectractor muscle, sb – space balloon, ten – tentacles, ts – tentacle sheath, tsm –

tentacle sheath musculature, or – orifice;

Figure 2
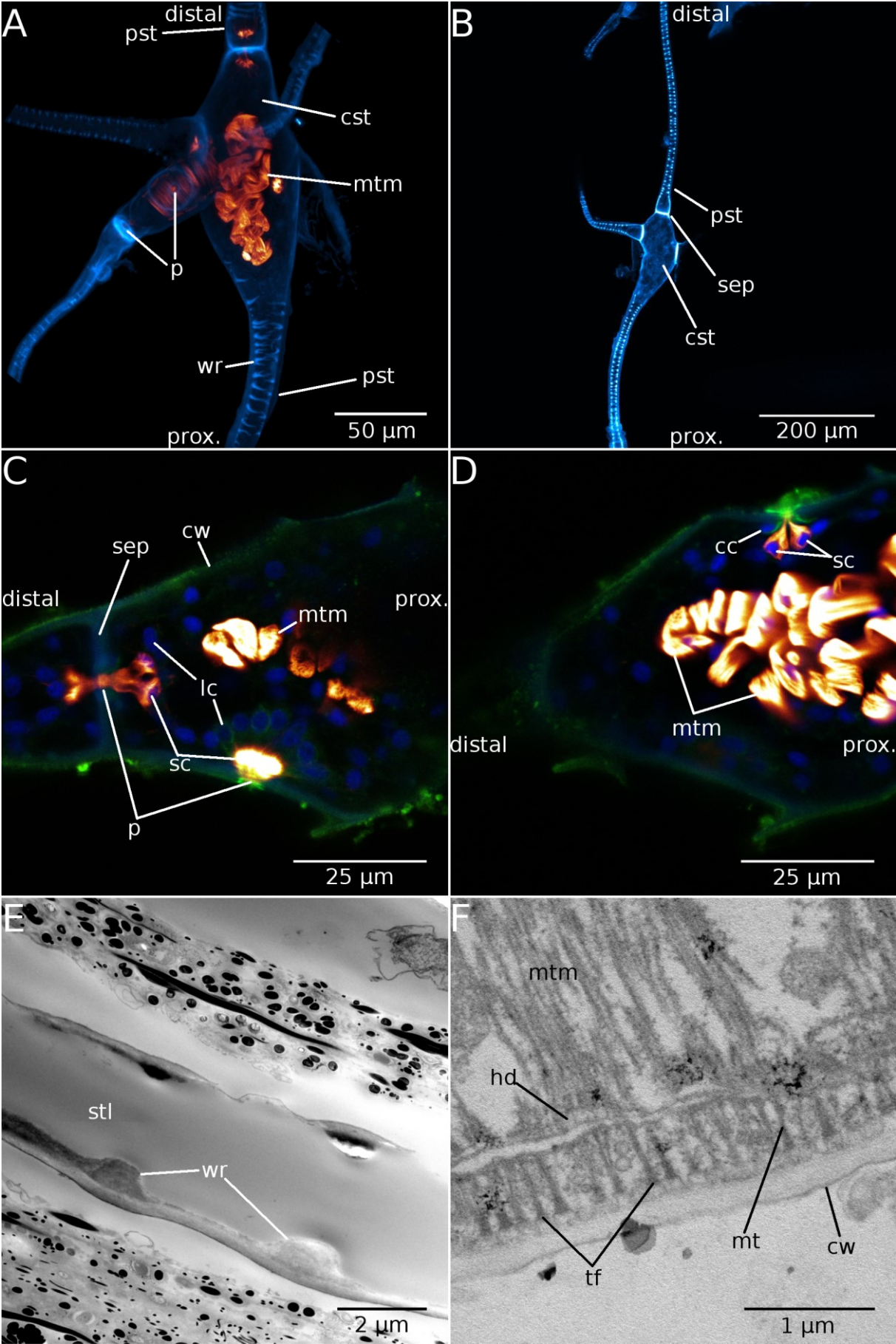
Fig. 2 – Stolons of *Hypophorella expansa*. A: Maximum intensity projection of a stolon capsule. Musculature in orange, cystid walls in blue. The median transversal muscle is positioned in the center of the distal stolon capsule. Stolons are separated via perforated septa. B: Maximum intensity projection of a stolon cystid. Cystid walls indicated in blue. Stolons are elongated at their proximal side and possess a small capsule-like expansion at their distal end. C: Maximum intensity projection of a stolon capsule. Musculature in orange, cell nuclei in blue and acetylated alpha-tubulin in green. D: Maximum intensity projection of a stolon capsule. Musculature in orange, cell nuclei in blue and acetylated alpha-tubulin in green. Adjacent stolons are separated by a septal disc, that is flanked by a cell complex which forms a rosette and acts as a transport epithelium. The outer layer of a rosette consists of a hemispherical arrangement of "limiting cells" that show a distinct alpha tubulin staining surrounding the cell nuclei. Proximal to the "limiting cells" are the "special cells" which show f-actin signal, project through the septal perforation and connect to the f-actin of the preceeding stolon. The cell lining of the perforation itself consists of "cincture cells" that show alpha tubulin signal projecting through the septal perforation. The median transversal muscle is also visible. E: TEM image of a longitudinal section of a stolon. The wrinkles show a higher electron density than the rest of the cystid wall. F: TEM image of a sagittal section through a stolon next to a piece of the *Chaetopterus* tube. The median transversal muscle is attached to a tendon cell at the base of the cystid wall. cc – cincture cell, cst – capsule of a stolon, cw – cystid wall, hd – hemidesmosomes, lc – limiting cell, mt – microtubule, mtm – median transversal muscle, p – septal perforation, pst – proximal side of a stolon, sc – special cell, sep – septal wall, stl – stolon lumen, tf – tonofilaments, wr – stolon wrinkle;

Figure 3
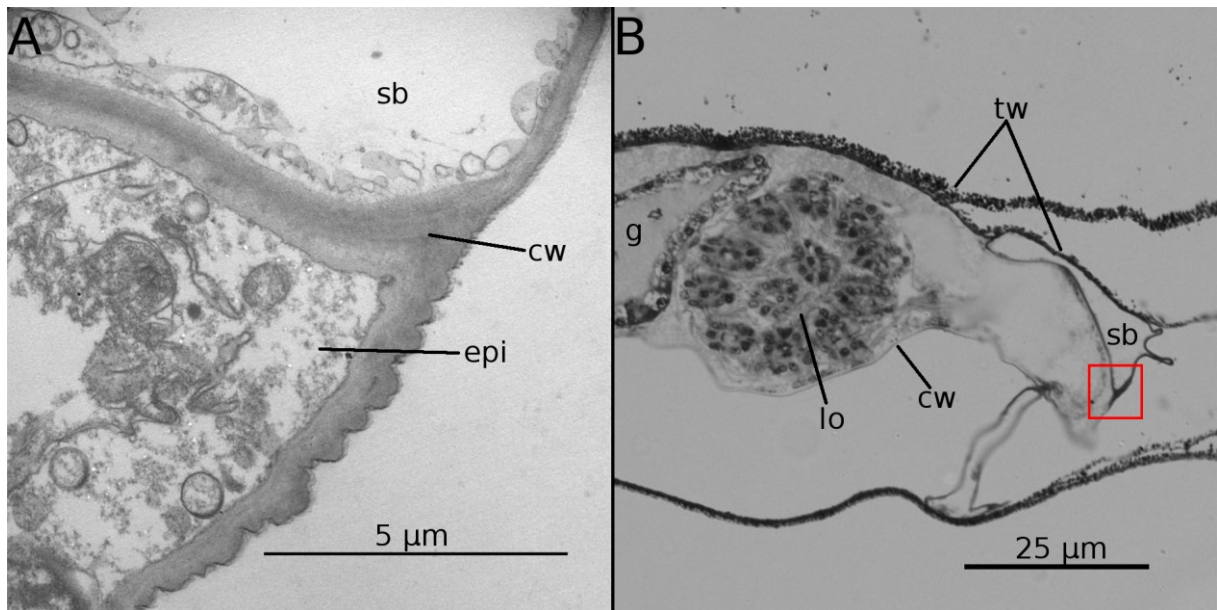
Fig 3 – Space balloon of *Hypophorella expansa*. A: TEM image of an ultrathin section (60 nm) of an autozooid at the border of regular cystid wall and a space balloon. The cystid walls show an epidermal layer, which is prominent below the regular cystid and delicate below the cystid wall of the space balloon. B: Semithin crosssection (1 µm) of an autozooid. The red square indicates the area of the ultrathin section of A. Note the collapsed form of the space balloon due to dehydration and embedding. cw – cystid wall, epi – epidermis, lo – lophophore, sb - space balloon, tw – *Chaetopterus* tube wall;

Figure 4
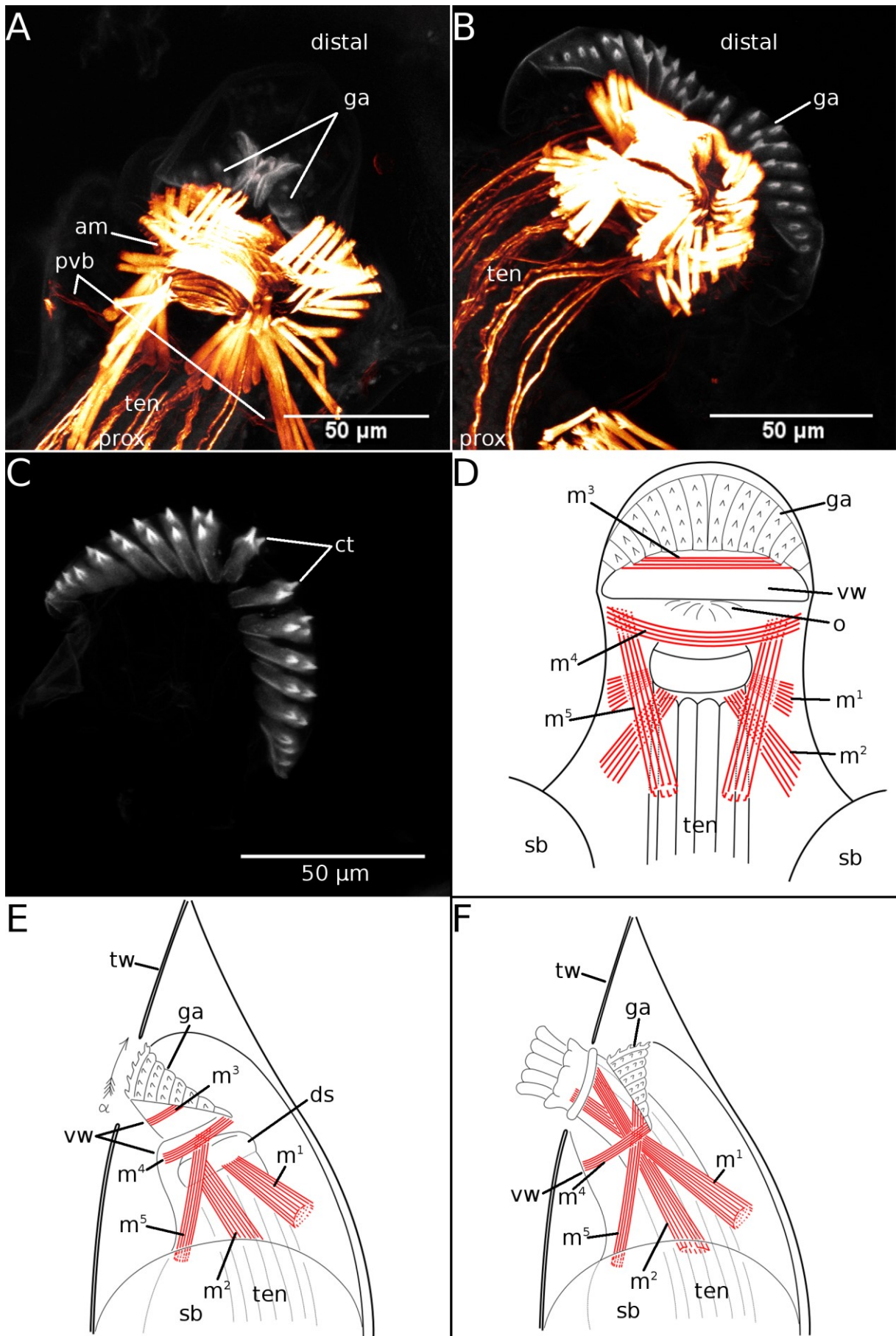
Fig. 4 – The gnawing apparatus of *Hypophorella expansa*. A-C: Maximum intensity projections of the apertural area. Musculature in orange, auto fluorescence in grey. D-F: Schematic drawings of the gnawing apparatus and associated apertural musculature (modified after Prouho, 1892). Musculature indicated in red. A: When the polypide is retracted the lateral sides of the distal gnawing apparatus are folded medially towards the orificial area. B: During the protusion process of the polypide, the lateral sides of the gnawing apparatus are lined up in a crecent moon shape. C: Chitinous elements of the gnawing apparatus when the polypide is protruded. Lateral-most columns of the bipartite gnawing apparatus possess one, median columns to two to three and median-most columns two spikes at their terminal ends. D: Frontal view on the apertural area of an autozooid with retracted polypide. In this scheme the muscle bundle m^3 directly inserts into the gnawing apparatus. It consists of two separate muscle bundles that insert medially into the gnawing apparatus, not laterally. E: Lateral view on the distal part of an autozooid with retracted polypide. Two muscle bundles that are associated with the gnawing apparatus, m^3 and m^4. m^4 constitutes vestibular wall musculature that is not directly associated with the gnawing apparatus. F: Lateral view on the distal area of an autozooid with protruded polypide. m^5 is shown to insert into the gnawing apparatus. Also note the that the muscle bundles m^2 and m^4 are shown to cross as they progress distally, in E they do not. am – apertural musculature, ct – chitinous tips of the columns of the gnawing apparatus, ds – diaphragmatic sphincter, ga – gnawing apparatus, m^{1-5} – muscle bundles of the apertural musculature, o – orifice, pvb – parietovaginal bands, sb – space balloon, ten – tentacles, tw – wall of the Chaetopterus tube, vw – vestibular wall;

Figure 5
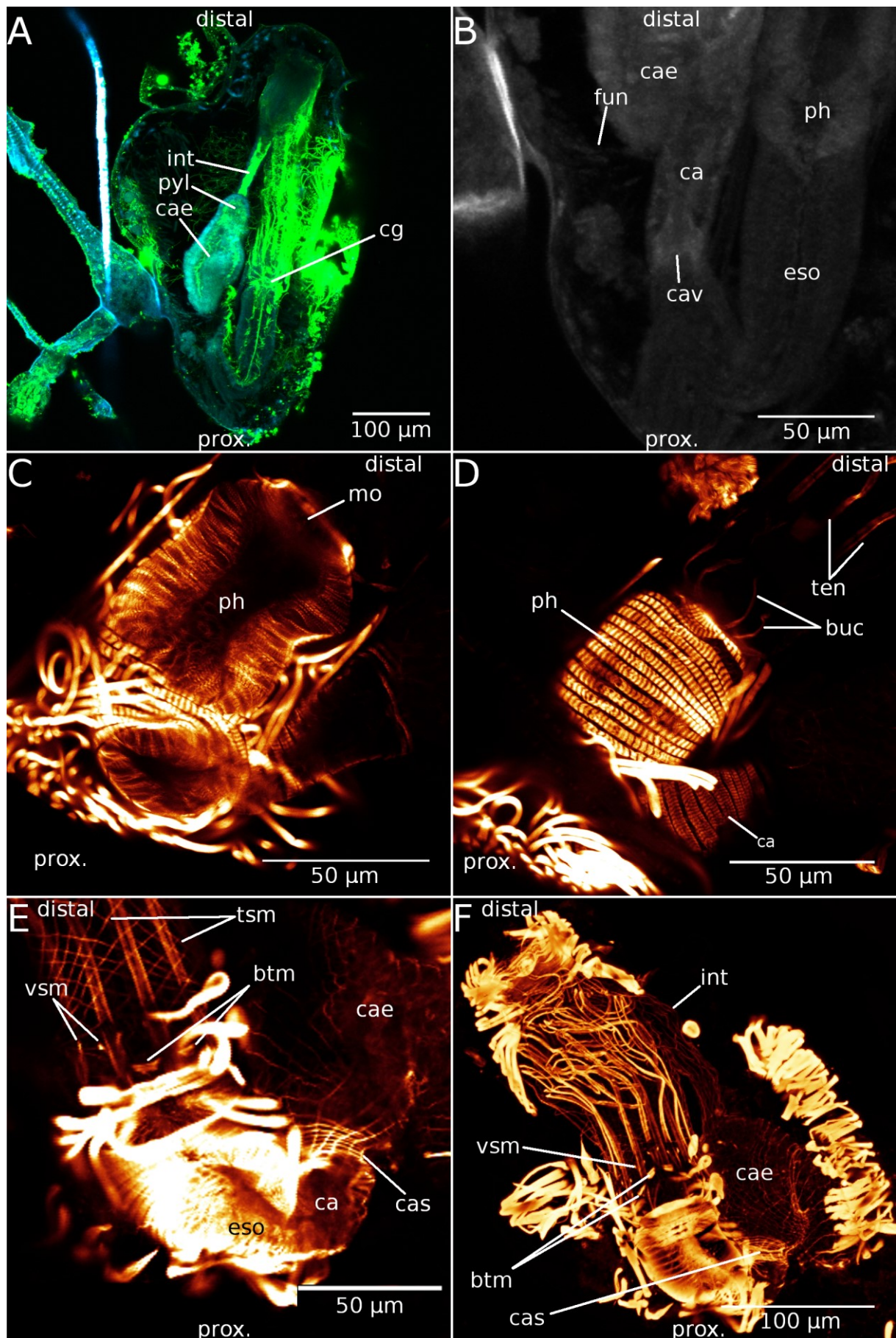
Fig. 5 – Digestive tract of *Hypophorella expansa*. Musculature in orange, cell nuclei in cyan, acetylated alpha-tubulin of nervous elements and cilia in green and autofluorescence of the gut in grey. A: A stolon with its corresponding autozooid. The digestive tract and especially the intestine show strong ciliation. B: Foregut of an autozooid. A short distal pharynx leads to an adjacent elongated esophagus. At its end the cardiac valve is visible, marking the transition from the esophagus to the cardia. The short tube-like cardia continues into the bulbous caecum, at which a very delicate funiculus is attached. It traverses the body cavity and inserts near the pore plate. C: The pharynx is a prominent myoepithelium and possesses mostly densely packed circular musculature. D: Buccal dilatators originate peri-orally and progress towards the proximal side of the tentacles. E: Tentacle sheath muscular net and the cardiac sphincter. F: The intestine solely consists of delicate longitudinal myofibrils. btm – basal transversal muscles, buc – buccal dilatators, ca – cardia, cae – caecum, cas – sphincter-like ring musculature of the cardia, cav – cardiac valve, cg – cerebral ganglion, eso – esophagus, fun – funicular strands, int – intestine, mo – mouth opening, ph – pharynx, pyl – pylorus, vsm – v-shaped muscles;

Figure 6
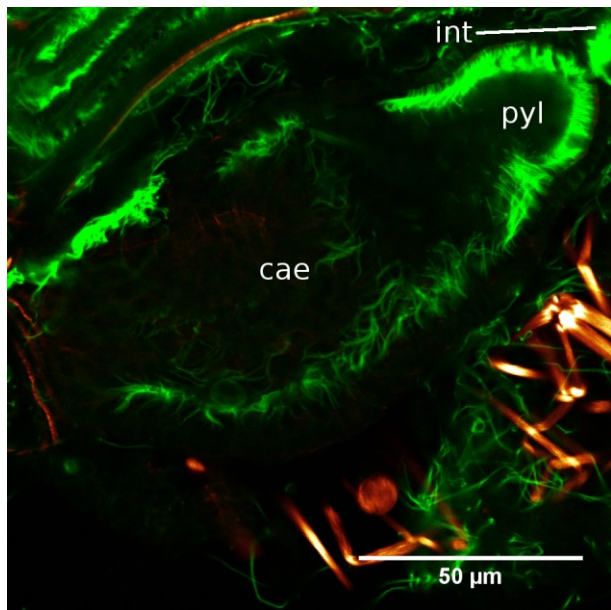
Fig. 6 – Optical section of the mid- and hindgut of *Hypophorella expansa*. Musculature indicated in orange, acetylated alpha-tubulin in green. The caecum shows a consistent ciliation that is not as prominent and dense as that of the adjacent pylorus and the terminal intestine. cae – caecum, int – intestine, pyl – pylorus;

Figure 7
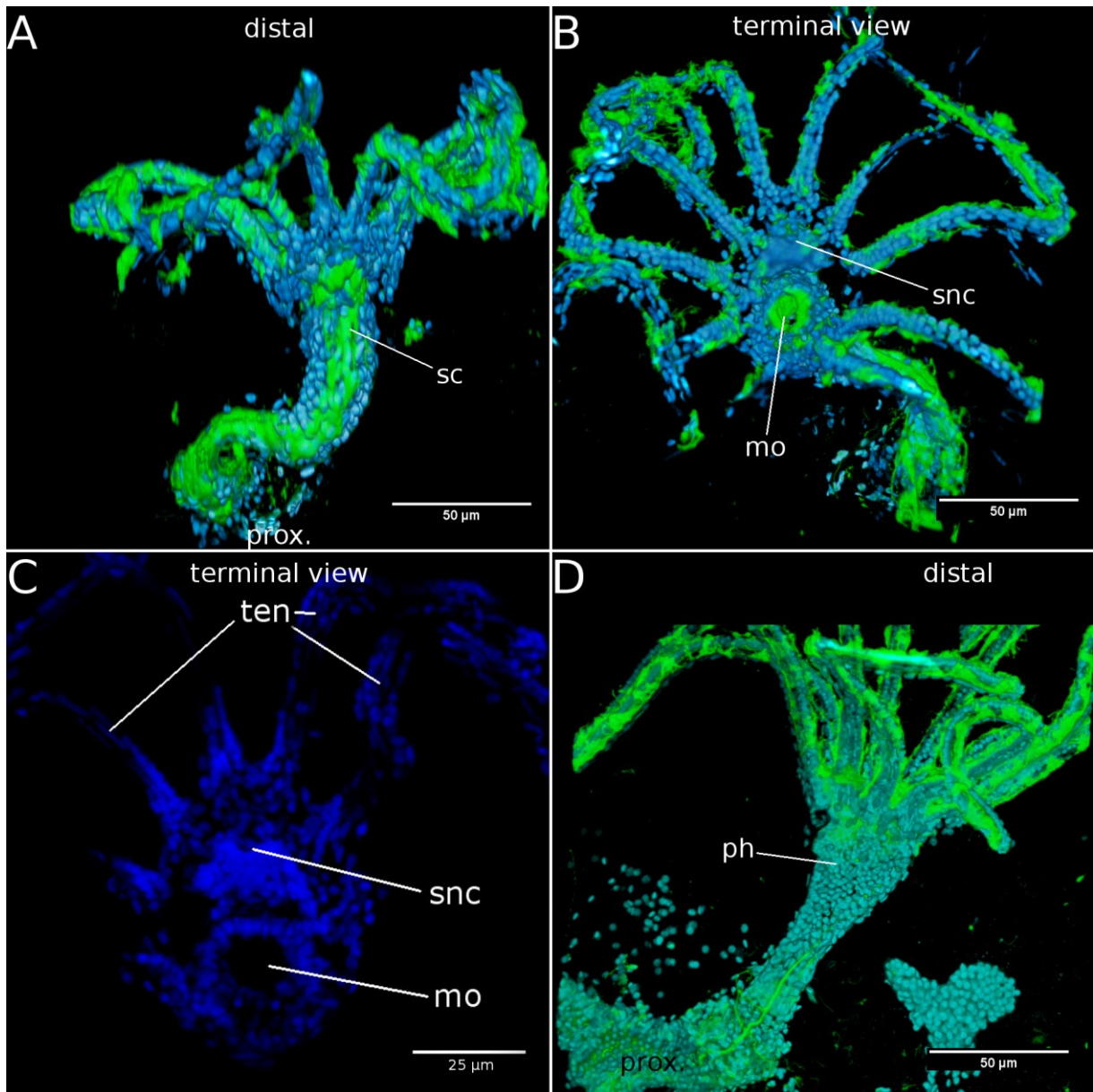
Fig. 7 – Lophophore of *Hypophorella expansa*. A + B: Volume renderings showing acetylated alpha-tubulin (green) and cell nuclei (cyan) of a protruded lophophore. In some autozooids longitudinal rows of cilia are present at the anal side of the pharynx that progress distally and terminate at the supraneural coelomopore. C: Nuclei (blue) of the lophophoral base in distal/terminal view. At the anal side next to the mouth opening a supraneural coelomopore is visible. D: An autozooid that does not possess a ciliary street or a supraneural coelomopore. mo – mouth opening, ph – pharynx, sc – ciliary street, snc – supraneural coelomopore, ten – tentacle;

Figure 8
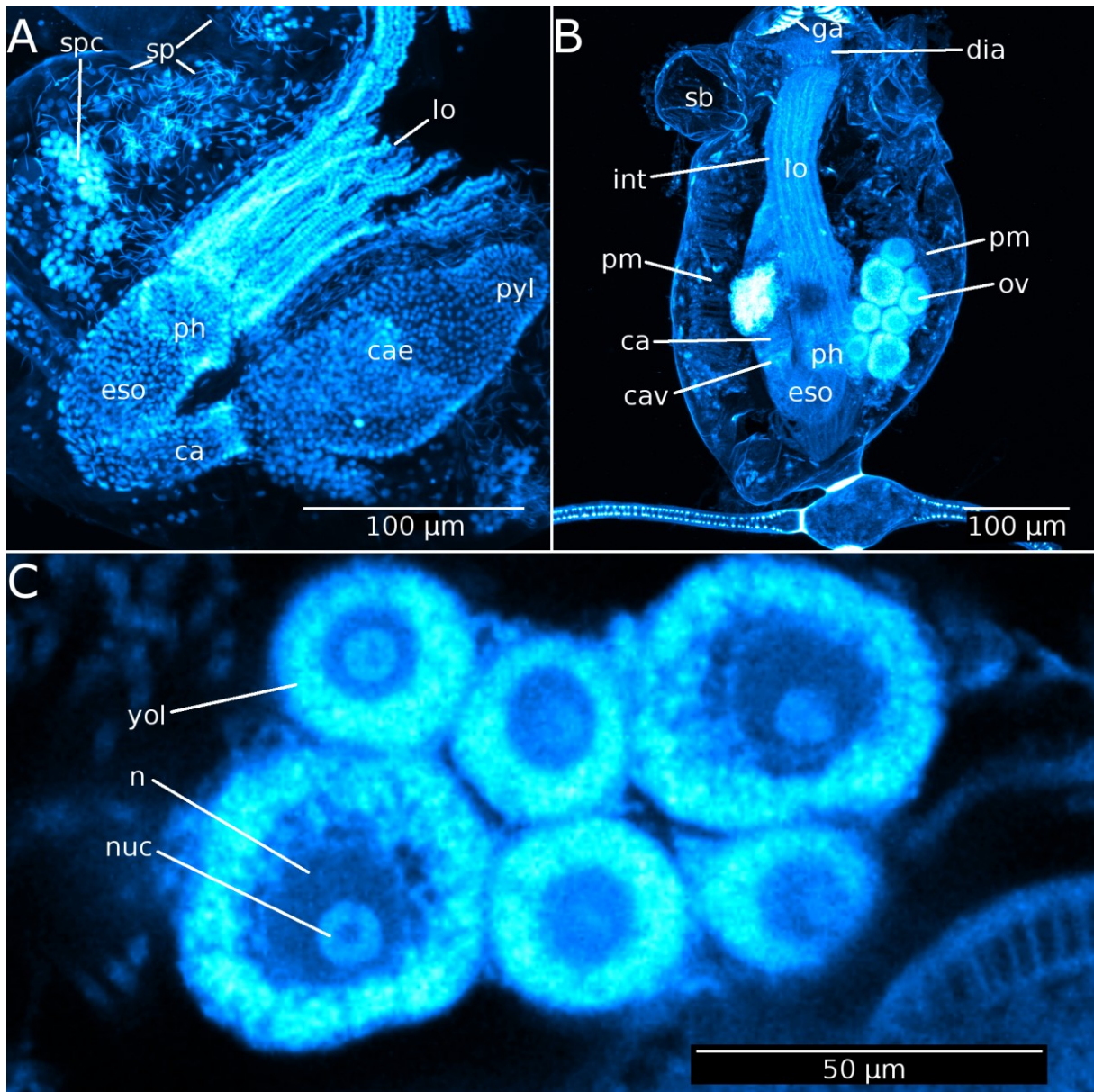
Fig. 8 – Gametes of *Hypophorella expansa*. Cell nuclei (A) and autofluorescense (B and C) in light blue. A: Sperm and clustered spermatogonia. A dissected autozooid with sperm and clustered spermatogonia is shown. The spermatogonia clusters are positioned in the proximo-lateral body cavity, while developed sperm are distributed throughout the body cavity. B: Ovarium of an autozooid. Maximum intensity projection of optical sections of an autozooid show developing oocytes at the lateral portion of an autozooid. C: Oocytes with an outer yolk layer. The cell nucleus with its nucleolus is surrounded by yolk. ca – cardia, cae – caecum, cav – cardiac valve, dia – diaphragm, eso – esophagus, ga – gnawing apparatus, int – intestine, lo –

lophophore, n – cell nucleus, nuc – nucleolus, ov – ovaries, ph – pharynx, pm – parietal muscles,

pyl – pylorus, sb – space balloon, sp – sperm, spc – cluster of developing sperm;

Figure 9
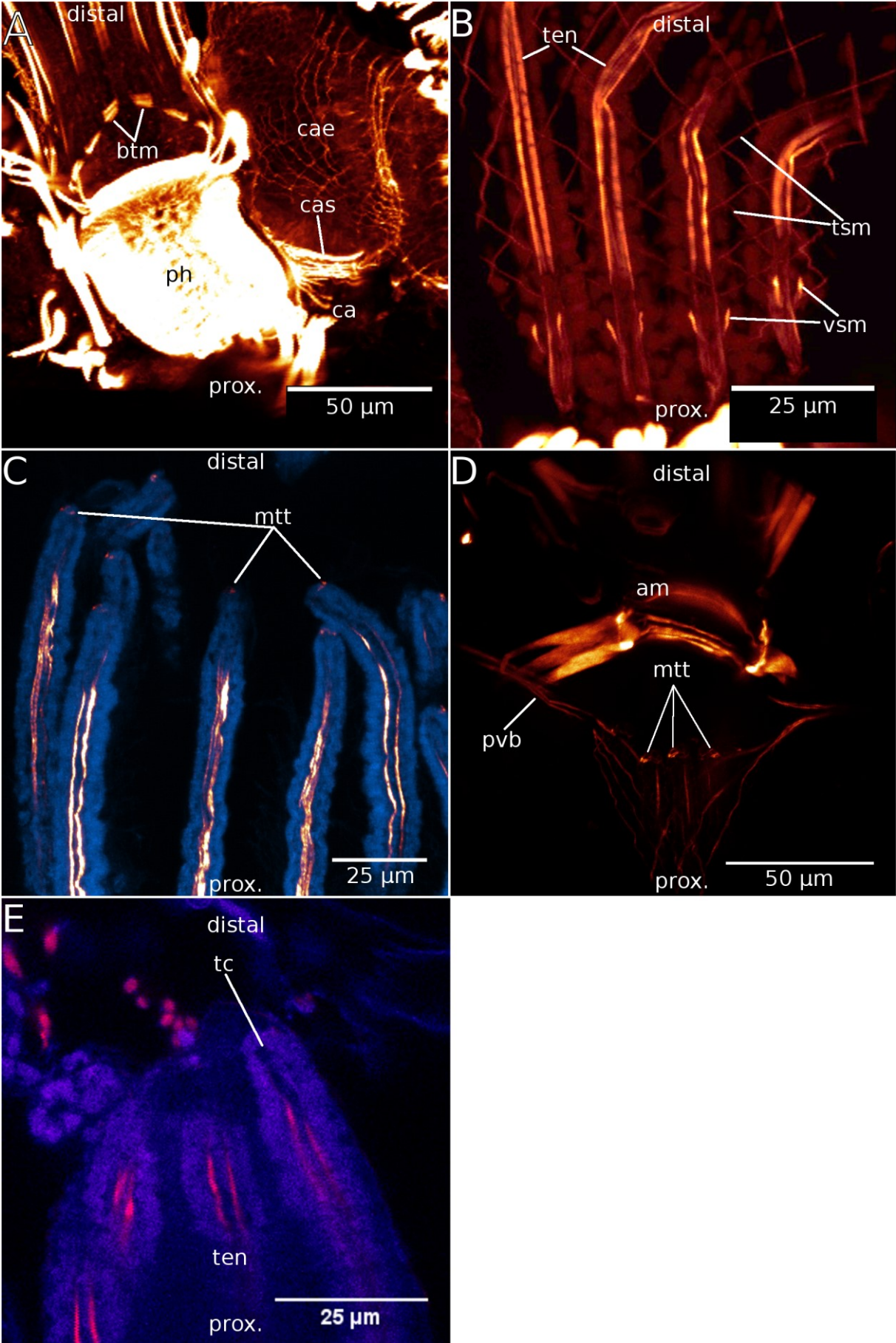
Fig. 9 – Maximum intensity projections of muscular elements of the lophophore of an autozooid of *Hypophorella expansa*. A: The lophophoral base, the fore- and the midgut are shown. Musculature in orange. The basal transversal muscles are positioned periorally, consisting of short smooth longitudinal myofibrils. B: Tentacle muscles and the muscular net inside the tentacle sheath. Musculature in orange. Each tentacle possesses two striated longitudinal muscles. At their proximal origin, V-shaped muscular tips are present. C: Distal parts of the tentacles. Musculature in orange, autofluorescence of tentacle epidermis in blue. Tentacles show muscular elements at their tips, separated from their longitudinal myofibrils. D: The apertural area, tentacle tips and distal tentacle sheath. Musculature in orange. The musculature of the tentacle tips consists of very delicate circular myofibrils. E: Tentacle coelom. Musculature in pink and cell nuclei in purple. The coelom in the tentacle tips is well visible distally to the longitudinal myofibrils of the tentacles. am – apertural musculature, btm – basal transversal muscles, ca – cardia, cas – sphincter-like circular myofibrils of the cardia, mtt – myofibrils of the tentacle tips, ph – pharynx, pvb – frontal parieto-vaginal bands, tc – tentacle coelom, ten - tentacle, tsm – tentacle sheath musculature, vsm – V-shaped muscles;

Figure 10
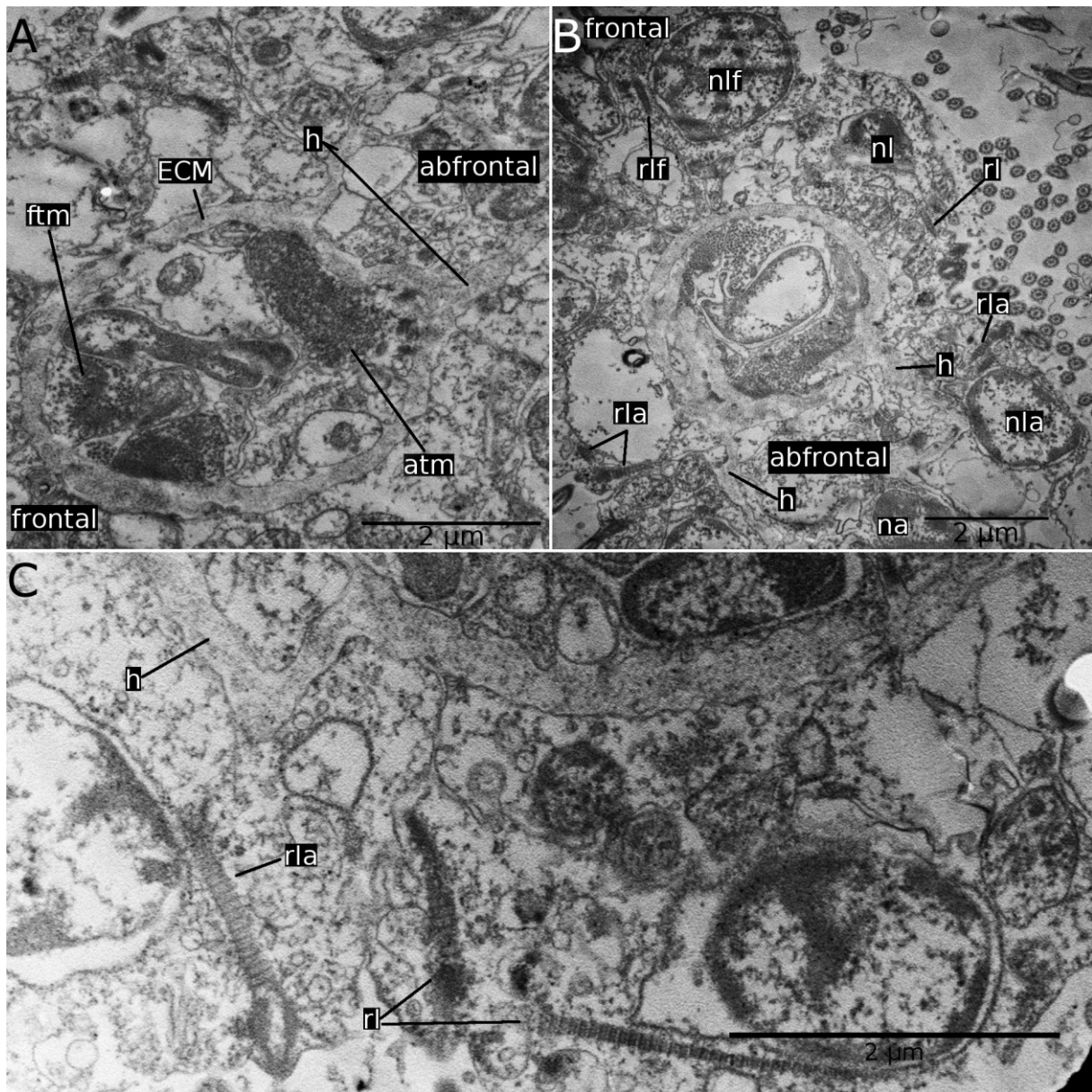
Fig. 10 – Tentacle ultrastructure of *Hypophorella expansa*. TEM-cross sections. A: Tentacle muscles. Each tentacle possesses two basiperitoneal longitudinal muscles, one abfrontal and one frontal tentacle muscle. B: Ciliary rootlets in epidermal tentacle cells. C: Ciliation of a tentacle. Several tentacle cells possess cilia, the latero-frontal cells, the lateral cells and the latero-abfrontal cells. atm – abfrontal tentacle muscle, ftm – frontal tentacle muscle, ECM – extracellular matrix, h – horns on the abfrontal side of the ECM, na – nucleus of an abfrontal cell, nl – nucleus of a lateral cell, nla – nucleus of a latero-abfrontal cell, nlf – nucleus of a latero-frontal cell, rl – rootlet of a lateral cilium, rla – rootlet of a latero-abfrontal cilium, rlf – rootlet of a latero-frontal cilium;

Figure 11
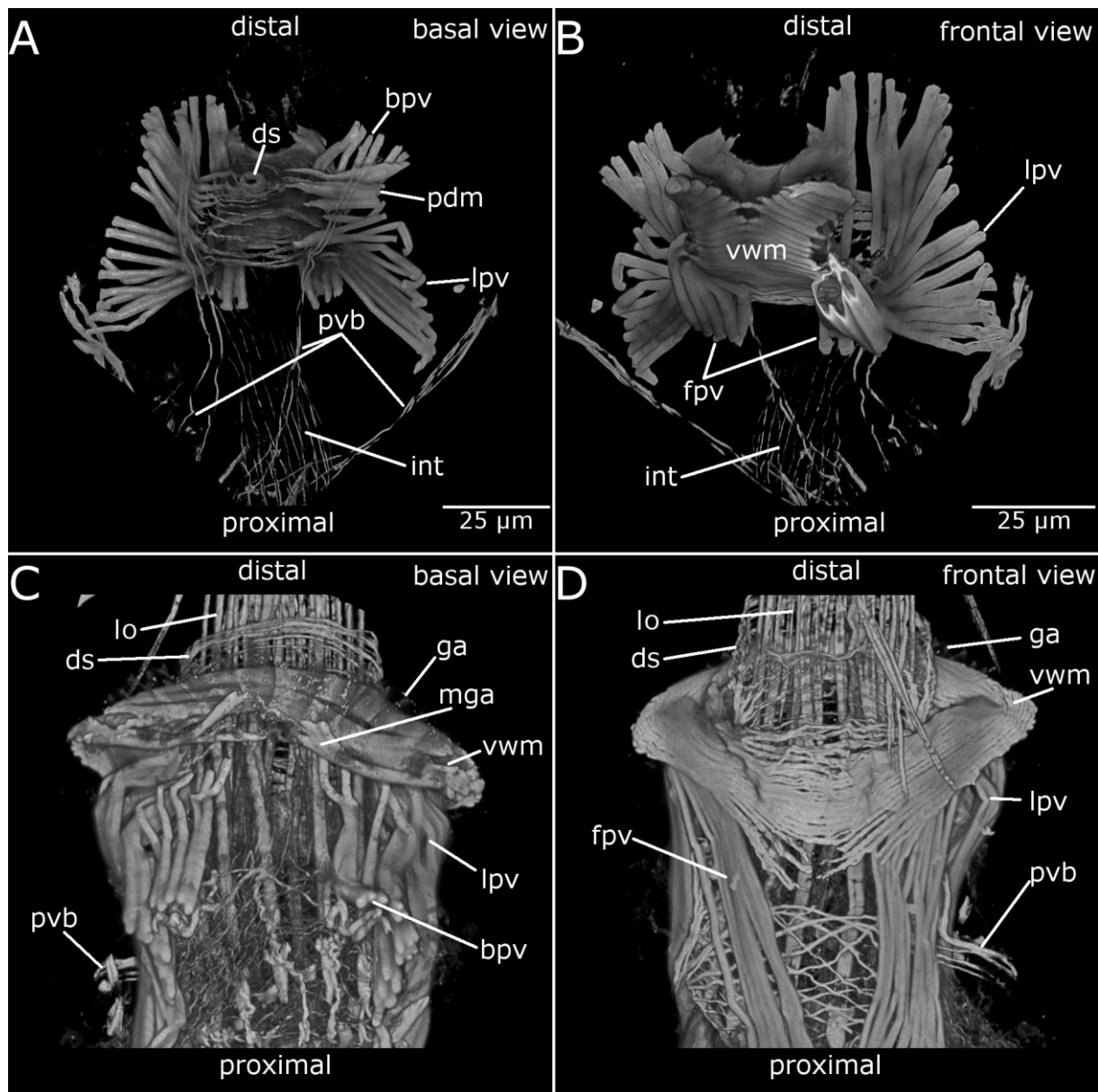
Fig. 11 – Volume renderings of the aperture musculature of *Hypophorella expansa*. F-actin in grey. A: Apertural area of a retracted polypide in basal view. The diaphragmatic sphincter is positioned basally of the vestibular wall muscles. B: The frontal side of the aperture of a retracted polypide. The prominent vestibular wall musculature consists of several tightly arranged ring muscles. C: Myoanatomy of the aperture in a semi-protruded lophophoral state in basal view. Two muscle bundles originate from the vestibular wall muscles laterally and insert at the gnawing apparatus. D: Apertural musculature of a semi-protruded polypide from a frontal view. The ring muscles of the diaphragmatic sphincter are positioned distally due to the half-protruded lophophore. bpv – basal parieto-vestibular muscles, ds – diaphragmatic sphincter, fpv –

frontal parieto-vestibular muscles, ga – gnawing apparatus, int – longitudinal myofibrils of the intestine, lo – lophophore, lpv – lateral parieto-vestibular muscles, mga – musculature associated with the gnawing apparatus, pdm – parieto-diaphragmatic muscles, pvb – parieto-vaginal bands, vwm – vestibular wall musculature;

Figure 12
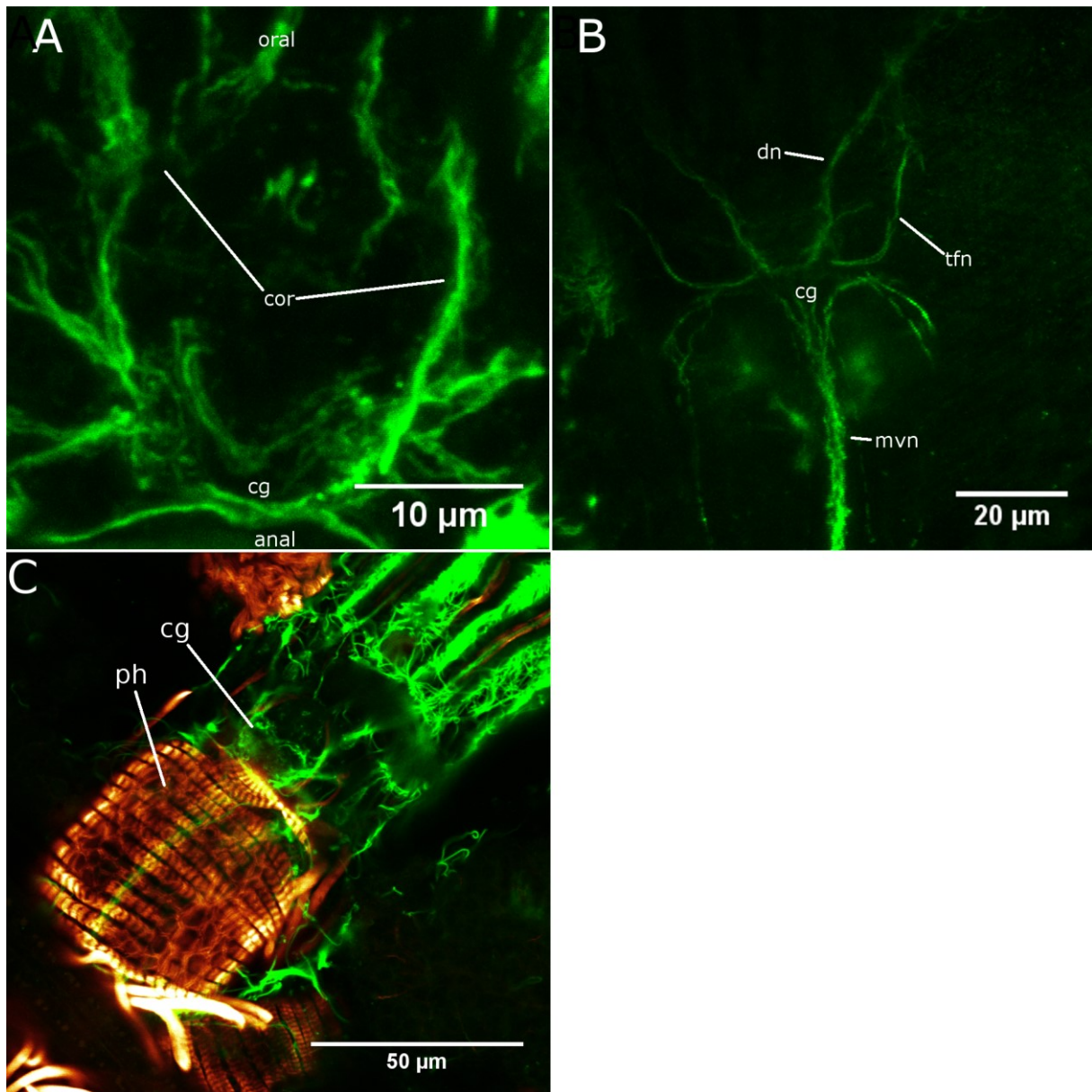
Fig. 12 – Gross morphology of the nervous system of the lophophoral base of *Hypophorella expansa*. Maximum intensity projections of the lophophoral base. Musculature in orange, acetylated alpha-tubulin in green. A: The cerebral ganglion on the anal side gives rise to the circum-oral nerve ring that engulfs the lophophoral base. B: The cerebral ganglion innervates the tentacle sheath with four prominent neurite bundles, the "direct nerves" on the median side and distal branches of the "trifid nerves" on the lateral side. They originate at the lateral side of the cerebral ganglion and split laterally, one part progressing distally, the other proximally to innervate retractor muscles and the lateral portions of the foregut. On the proximal side, the cerebral ganglion gives rise to the prominent medio-visceral nerve that continues proximally

along the pharynx to the cardiac valve. C: The cerebral ganglion is positioned on the anal side at the lophophoral base. cor – circum-oral nerve ring, cg – cerebral ganglion, dn – direct nerve of the tentacle sheath, mvn – medio-visceral nerve, ph - pharynx, tfn – distal branch of the trifid nerve;

Figure 13
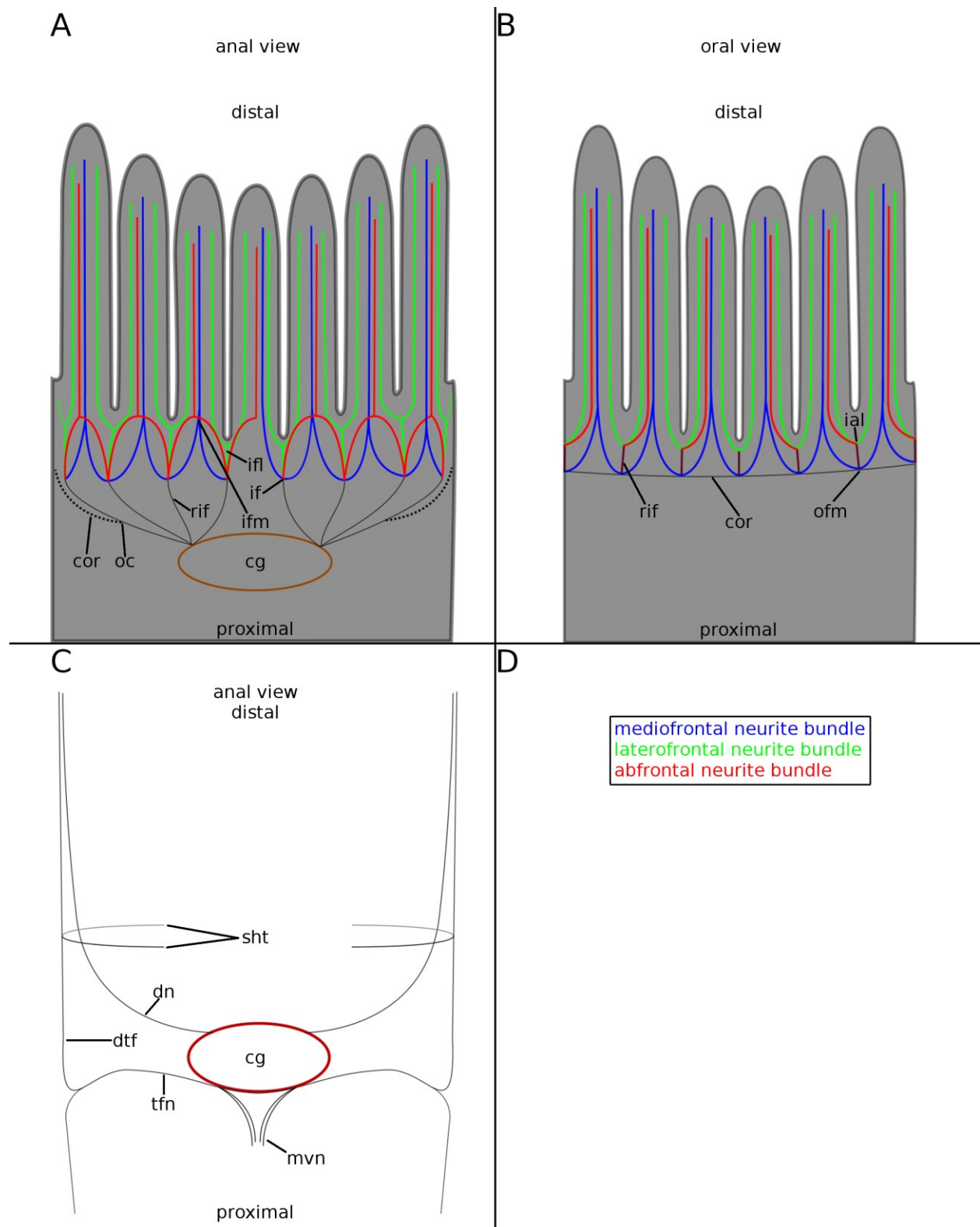
Fig. 13 – Tentacle sheath and tentacle innervation pattern of the lophophore of *Hypophorella expansa*. Schematic drawings of the tentacle innervation and nerve origins of the tentacles on the anal and oral side of the lophophore. A: Tentacle innervation on the anal side of the lophophore. The cerebral ganglion is the center of the nervous system positioned at the anal side of the lophophoral base. On its disto-lateral edges, four prominent neurite bundles originate on the left and the right side each. Each neurite bundle gives rise to a root of intertentacular forks, from which the tentacle neurite bundles originate. The medio-frontal and abfrontal tentacle neurite bundles of the median-most tentacle is supplied by one neurite bundle only. The medio-frontal neurite bundle has its origin on the median-most neurite bundle originating directly from the cerebral ganglion, the abfrontal nerve from the left neurite bundle. The lateral-most neurite bundle from the cerebral ganglion also gives rise to the circum-oral nerve ring that innervates the tentacles on the oral side. B: Tentacle innervation on the oral side of the lophophor. The circum-oral nerve ring innervates all tentacles and provides them with two latero-frontal, one medio-frontal and one abfrontal neurite bundle. The medio-frontal neurite bundle comprises two fused neurite bundles originating from the circum-oral nerve ring in intertentacular position. From this position, an additional neurite bundle progresses distally over a short distance and splits into three neurite bundles, two of them innervate two neighboring tentacles with one latero-frontal neurite bundles each and (from the left side to median) the tentacle to the right with one abfrontal neurite bundle. On the right side the tentacles are supplied with on abfrontal neurite bundle each from the right intertentacular fork. C: The innervation of the tentacle sheath emerges from the cerebral ganglion. The "direct nerve" orginates from the disto-lateral part of the ganglion. The second pair of tentacle sheath neurite bundles (i.e. "trifid nerve") arises from the proximal side of the cerebral ganglion, continues laterally, bends towards the pharynx, bifurcates and gives rise to the distal branches of the "trifid nerve", that continue distally over a short distance where they split again. One branch continues distally and the other produces two neurite bundles that partially encircle the tentacle sheath. The anal ramification also connects to the crossing "direct

nerve". At the lateral bifurcation at the level of the cerebral ganglion the second branch of the "trifid nerve" turns proximally and innervates the lateral walls of the pharynx. cg – cerebral ganglion, cor – circum-oral nerve ring, dn – "direct nerve" of the tentacle sheath, dtf – distal branch of the "trifid nerve", ial – intertentacular fork of the abfrontal and latero-frontal tentacle neurite bundles, if – intertentacular fork, ifl – intertentacular fork of the latero-frontal tentacle neurite bundles, ifm – merging point of neurite bundles originating from the intertentacular fork to create the medio-frontal neurite bundle, mvn – medio-visceral nerve, oc – origine of the circum-oral nerve ring, rif – neurite bundle that gives rise to a intertentacular fork, sht – perpendicular branch of the distal "trifid nerve" portion of the tentacle sheath nerve;

Figure 14
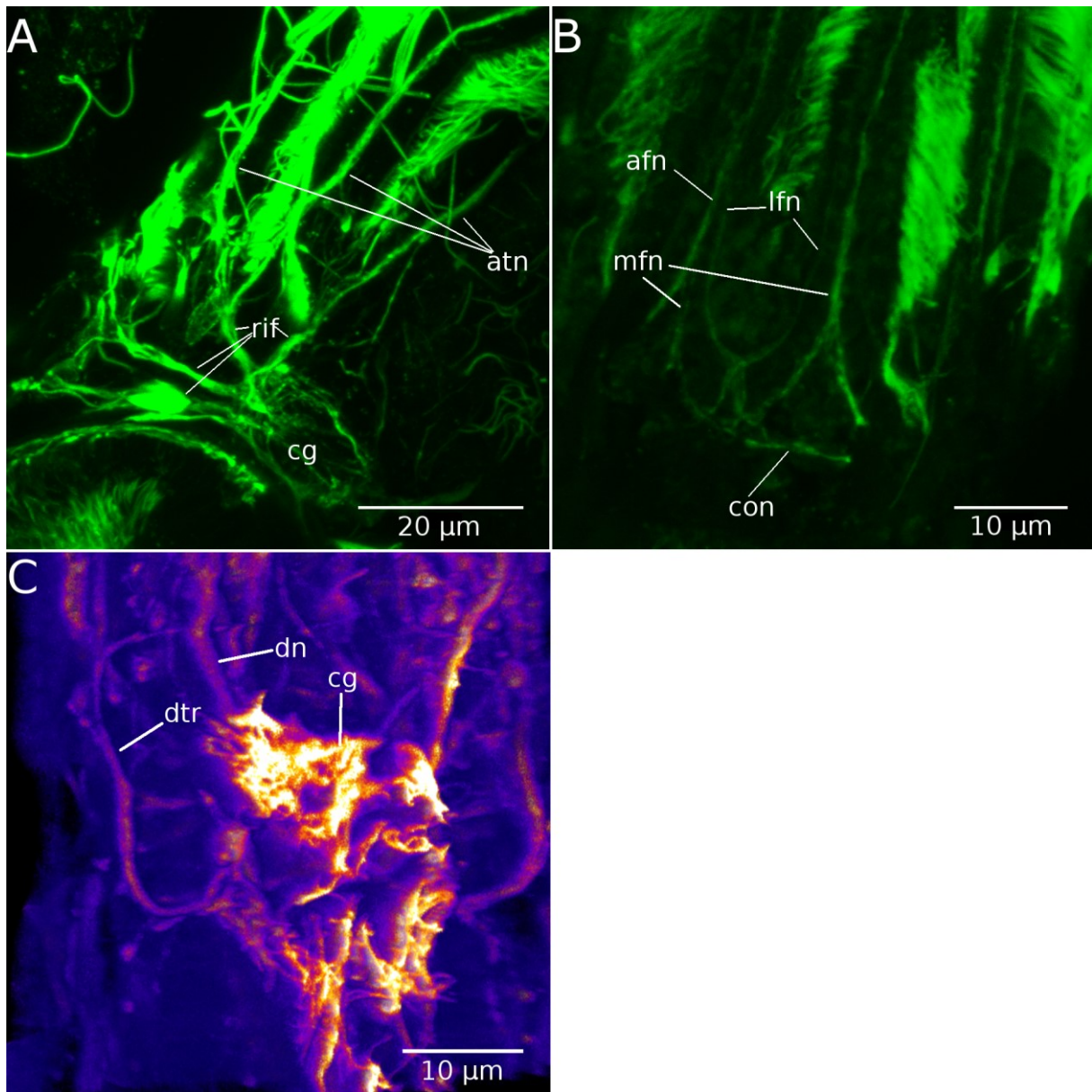
Fig. 14 – Gross neuro-anatomy of the lophophoral base. Maximum intensity projections of the lophophoral base on the anal (A, C) and oral side (B), respectively. Acetylated alpha-tubulin in green (for A, B and C). A: On the anal side, the cerebral ganglion gives rise to four prominent neurite bundles on each latero-distal side that further innervate the tentacles. The lateral-most neurite bundle also gives rise to the circum-oral nerve ring. B: On the oral side, the tentacles are supplied with neurite bundles that arise from the circum-oral nerve ring. C: Tentacle sheath innervation. The "trifid nerves" originate at the baso-lateral sides of the cerebral ganglion. They continue laterally, bend towards the pharynx and then distally, where they split into two neurite bundles and partially encircle the tentacle sheath. The nervous branches on the anal side further

connect with the "direct nerves", creating the compound "tentacle sheath nerves" that progress distally. atn – abfrontal tentacle nerve, cg – cerebral ganglion, con – circum-oral nerve ring, dn – direct nerve, lfn – latero-frontal tentacle nerve, mfn – medio-frontal tentacle nerve, rif – neurofibril with the intertentacular fork at its distal end, sh.tr – part of the trifid nerve that splits up distally and encircles the tentacle sheath, tfn – trifid nerve;

Figure 15
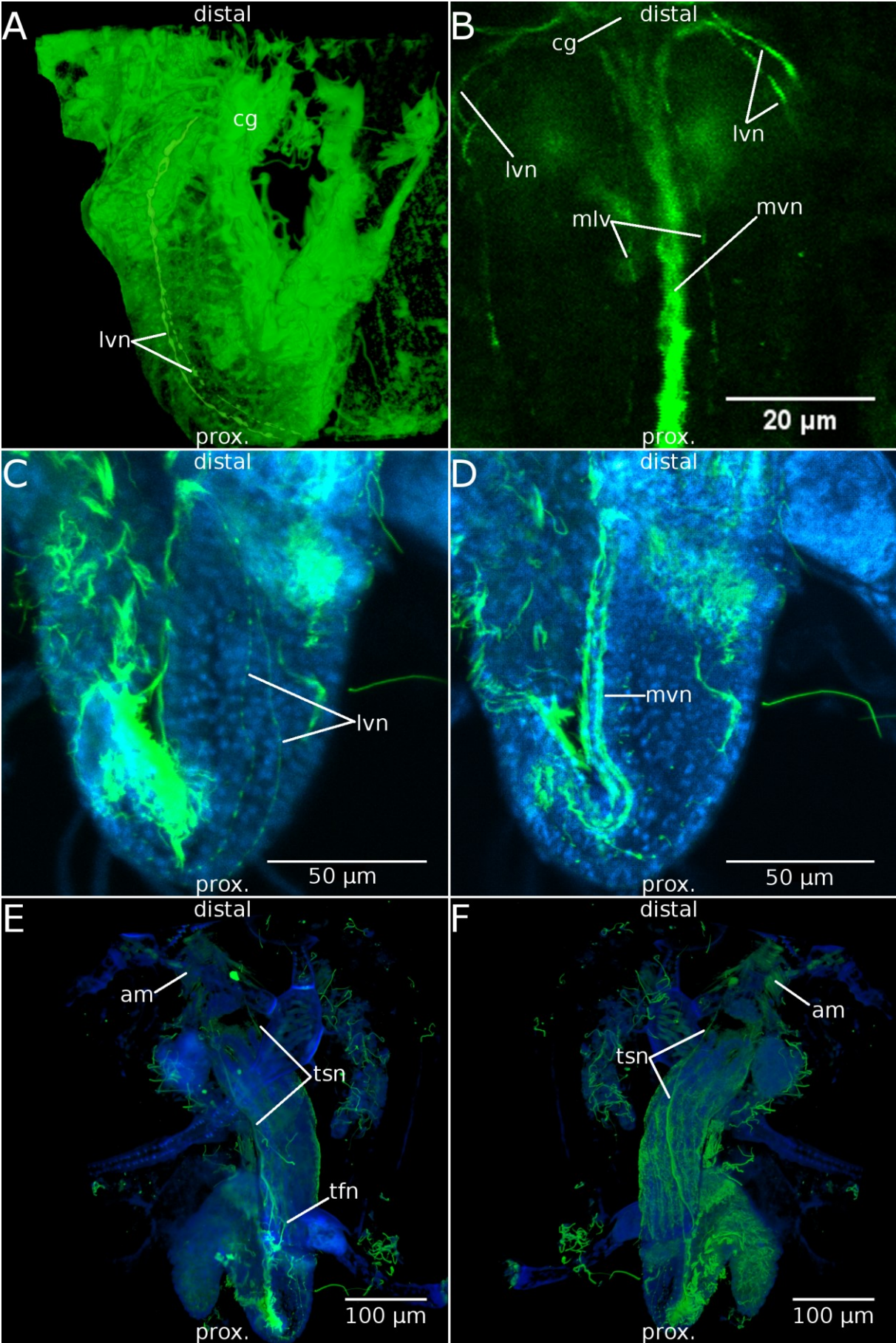
Fig. 15 – Visceral innervation and tentacle sheath nerves of *Hypophorella expansa*. Acetylated alpha-tubulin in green. A: Volume rendering of the two latero-visceral neurite bundles of the pharynx. B: Maximum intensity projection of the foregut. The foregut possesses two latero-visceral neurite bundles, a prominent medio-visceral neurite bundle, and two lateral medio-visceral neurite bundles. C+D: Progression of the visceral innervation. Cell nuclei in cyan, acetylated alpha-tubulin in green. C: Two latero-visceral nerves originate from the cerebral ganglion and progress laterally and proximally and continue along the lateral side of the foregut towards the cardiac valve. D: The mediovisceral neurite bundle arises from the cerebral ganglion and continues proximally on the anal side of the pharynx towards the cardiac valve. E: Maximum intensity projections of a dissected autozooid. Cell nuclei in blue, acetylated alpha-tubulin in green. The progression of the compound tentacle sheath nerves towards the aperture. F: The progression of the compound tentacle sheath nerves towards the aperture. Cell nuclei in blue, acetylated alpha-tubulin in green. am – aperture musculature, cg – cerebral ganglion, mlv – medio-lateral visceral neurite bundles, lvn – latero-visceral neurite bundles, mvn – medio-visceral neurite bundle, tfn – distal branch of the "trifid nerve", tsn – compound tentacle sheath nerve;

Figure 16
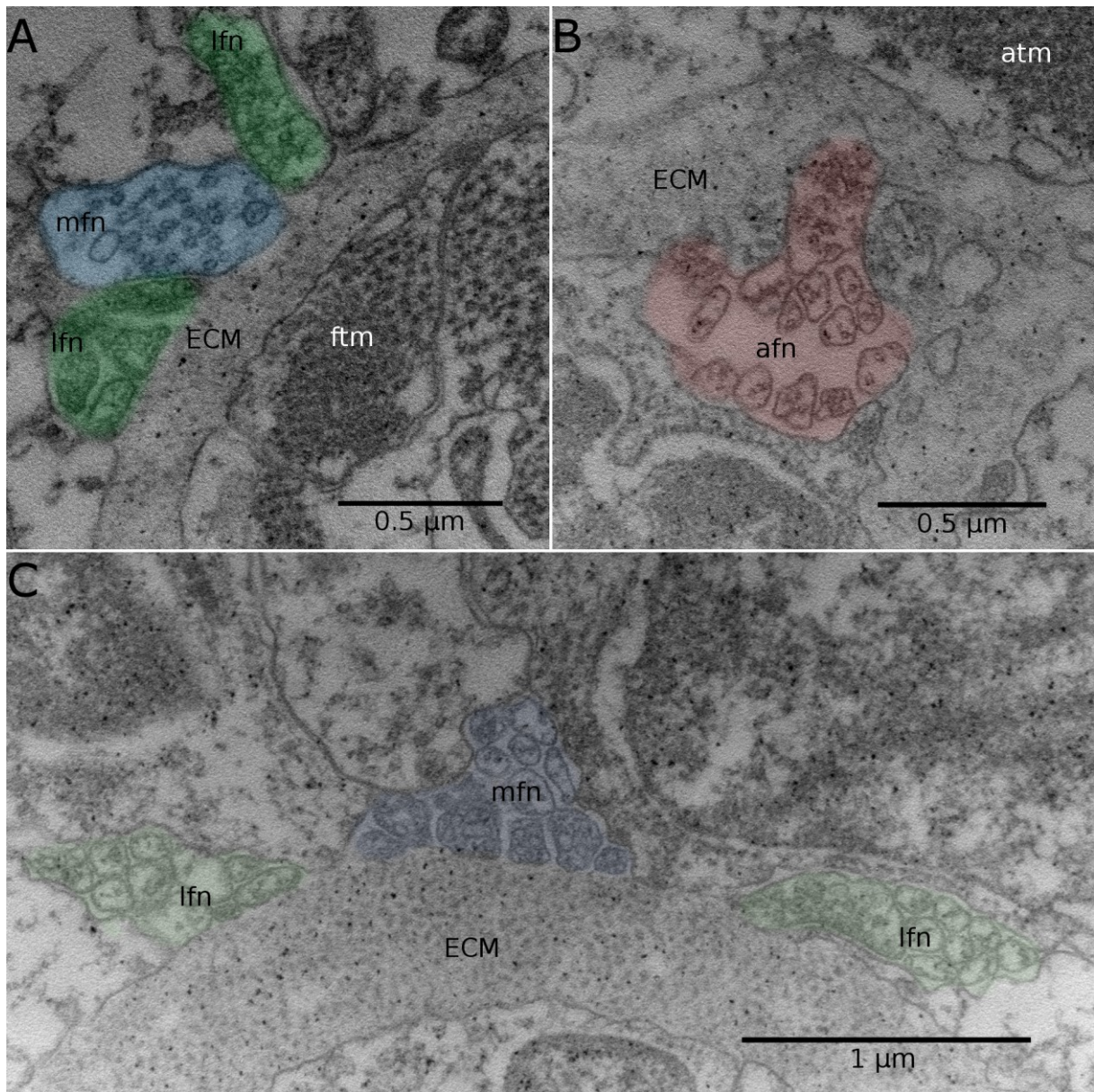
Fig. 16 – Tentacle neurite bundles of *Hypophorella expansa*. TEM images of tentacle cross sections. A: The frontal side of the distal portion of a tentacle. Three bordering basiepidermal frontal tentacle neurite bundles are visible, the medio-frontal tentacle neurite bundle (in blue) and two flanking latero-frontal tentacle neurite bundles (in green). B: Abfrontal side of a tentacle. The abfrontal tentacle neurite bundle is marked in red. C: Proximal part of a tentacle. Basiepidermal tentacle neurite bundles are further apart as in A, showing that the lateral distance between the tentacle neurite bundles gets smaller while they progress distally. afn – abfrontal tentacle nerve, ECM – extracellular matix, ftm – frontal longitudinal muscle of a tentacle, lfn – latero-frontal tentacle nerve, mfn – medio-frontal tentacle nerve;

Figure 17
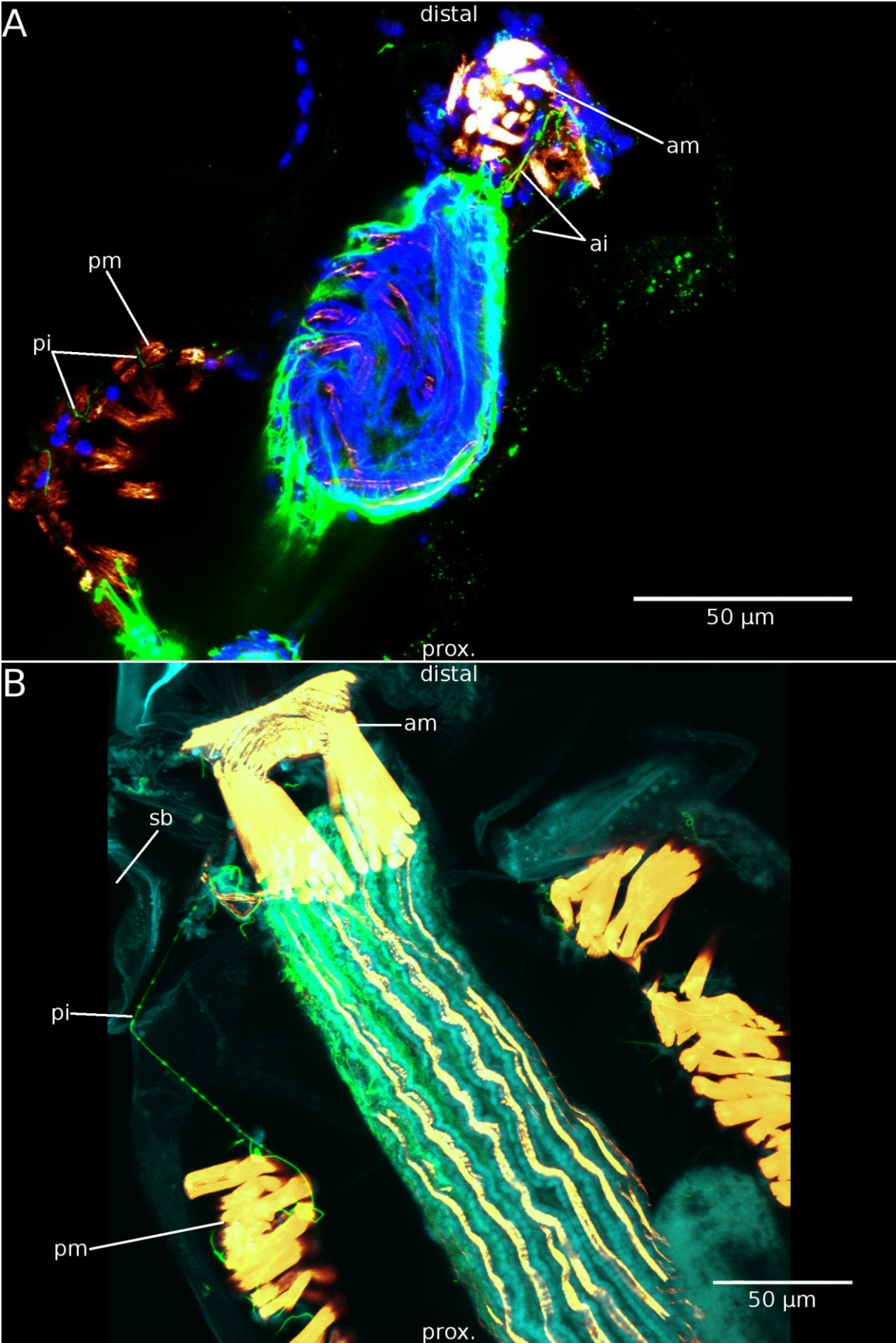
Fig. 17 – Apertural and parietal innervation of an autozooid of *Hypophorella expansa*. A: Apertural innervation. Musculature in orange, cell nuclei in blue and acetylated alpha-tubulin in green. Two neurite bundles extend along the tentacle sheath and innervate the distal apertural musculature. B: Parietal innervation. A neurite bundle from the tentacle sheath projects along the frontal parieto-vaginal band towards the proximal base of the space balloon where it bends proximally and continues along the frontal body wall towards the parietal muscles, innervating them in a meandering manner. ai – neurite bundles innervating the apertural area, am – aperture musculature, pi – neurite bundles innervating the parietal muscles, pm – parietal muscles, sb – space balloon, ten – tentacles;

Figure 18
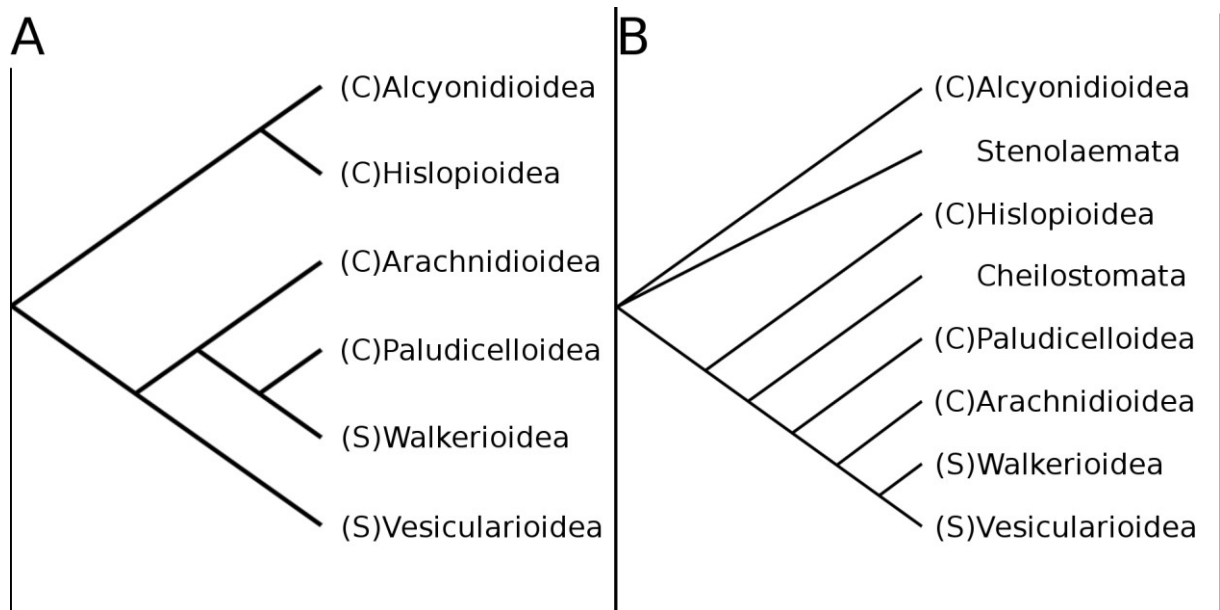
Fig. 18 – Phylogenetic scenarios of the interrelationship of ctenostome "superfamilies" with a "carnosan" (C) and "stoloniferan" (S) colony type. A: Phylogenetic tree based on Jebram (1986). B: Phylogenetic tree based on Todd (2000). Stenolaemata is considered the sister group of Gymnolaemata ("Ctenostomata" + Cheilostomata), while the monophyletic Cheilostomata is considered to have evolved from a ctenostome ancestor, Ctenostomata is therefore considered paraphyletic.

Zusammenfassung

Bryozoa (=Ectoprocta) ist eine artenreiche Klasse innerhalb der Lophotrochozoa, bestehend aus koloniebildenden, im Wasser lebenden Filtrierern. Die minierende ctenostome Bryozoe *Hypophorella expansa* lebt in pergamentartigen Wohnröhren von Polychaeten. Die Untersuchung möglicher morphologischer Adaptationen bezüglich ihrer Lebensweise und des einzigartigen Lebensraumes verlangt nach einer detaillierten morphologischen Analyse. Hierfür wurden Immunofärbungen in Kombination mit konfokaler Laser-Scanning-Mikroskopie (engl. confocal laser scanning microscopy, CLSM), histologische Techniken und Transmissionselektronenmikroskopie (TEM) verwendet. Das Grundgerüst einer Kolonie von *H. expansa* besteht aus länglichen Stolonen mit distaler kapselartiger Erweiterung ihrer Zystidwände, in denen sich ein medianer Transversalmuskel befindet. Zusätzlich ist lateral je ein Autozooid diesen kapselartigen Erweiterungen angegliedert. Die Zystidwände der Autozooide besitzen zwei kugelige, fronto-laterale Strukturen („space balloons"), die für ausreichenden Raum zwischen den Röhrenschichten sorgen. Zum Perforieren dieser Röhrenschichten besitzt ein jedes Autozooid am distalen Ende einen Rapselapparat. Die Tentakelscheide beherbergt ein Netz aus helikoidal verlaufenden, sich überkreuzenden, longitudinalen Muskelfasern, die von der Lophophorbasis aus distal entlangziehen und sich zu vier parieto-vaginalen Bändern vereinigen. Der Verdauungstrakt besteht aus einem myoepithelialen Pharynx, einem kurzen Ösophagus, einer kurzen Cardia, einem knollenförmigen Caecum, einem länglichen Intestinum und einem distal terminierenden Anus. Das Cerebralganglion liegt analseitig und innerviert Tentakelscheide, Lophophor und Vorderdarm. Dem Ganglion entspringen vier Neuritbündel der Tentakelscheide, die sich distal zu zwei Neuritbündeln vereinigen. Ebenfalls vom Cerebralganglion ausgehend wird jeder Tentakel von vier frontalen und einem abfrontalen Neuritbündel innerviert. Die Wuchsform der Kolonie ermöglicht eine rasche Kolonisierung der

Polychaetenröhre. Das helikoidale Muskelfasernetz der Tentakelscheide hat möglicherweise einen ähnlichen stabilisierenden Effekt wie bei Phylactolaematen, ohne jedoch zusätzliche Ringmuskulatur zu benötigen. Die mit dem Raspelapparat assoziierten Muskelfasern sind möglicherweise zu den Muskelfasern der Vestibularwand homolog. Die Innervierung der Tentakelscheide evoluierte offenbar ausgehend von kurzen Neuritbündeln, die sich innerhalb der Phylacotaematen in einen Nerven-Plexus auflösen, hin zu zwei Neuritbündeln der Tentakelscheide, die sich bei Gymnolaematen über die gesamte Länge der Tentakelscheide erstrecken. Die medio-lateralen, visceralen Neuritbündel bei Ctenostomen sind möglicherweise homolog zu den medio-lateralen Neuritbündeln bei Phylacolaematen. Ausgehend von den diskutierten Daten besaß der letzte gemeinsame Vorfahre von Gymnolaemata allen Anschein nach zwei gestreifte Muskelfasern je Tentakel, parieto-vaginale Bänder, einen myoepithelialen Pharynx, longitudinale Muskelfasern des Intestinums, einen proximal terminierenden Anus, eine geringe Anzahl an Neuritbündeln der Tentakelscheide die in weiterer Folge die Apertur und die Parietalmuskeln innervierten, vier Neuritbündel je Tentakel, von denen das mediofrontale Bündel direkt dem circum-oralen Nervring entsprang und ein medio-viscerales Neuritbündel des Vorderdarms.